Monthly Notices
of the
ROYAL ASTRONOMICAL SOCIETY

MNRAS **433,** 2–22 (2013)
Advance Access publication 2013 May 29

doi:10.1093/mnras/stt647

One year of monitoring of the Type IIb supernova SN 2011dh

D. K. Sahu,[1]⋆ G. C. Anupama[1] and N. K. Chakradhari[2]

[1]*Indian Institute of Astrophysics, Koramangala, Bangalore 560 034, India*
[2]*Pt. Ravi Shankar Shukla University, Raipur, India*

Accepted 2013 April 14. Received 2013 April 2; in original form 2013 January 23

ABSTRACT

Optical *UBVRI* photometry and low-resolution spectroscopy of the Type IIb supernova SN 2011dh in M51 are presented, covering the first year after the explosion. The light curve and spectral evolution are discussed. The early phase light-curve evolution of SN 2011dh is very similar to SN 1993J and SN 2008ax. In the late phase, however, SN 2011dh declines faster than SN 1993J. The late phase decline in the *B* band is steeper than in the *R* and *I* bands, indicating the possibility of dust formation. With a peak *V*-band absolute magnitude of $M_V = -17.123 \pm 0.18$ mag, SN 2011dh is a marginally faint type IIb event. The reddening corrected colour curves of SN 2011dh are found to be redder than other well-studied Type IIb supernovae. The bolometric light curve indicates $\sim$0.09 $M_\odot$ of ^{56}Ni is synthesized during the explosion. The He I lines were detected in the spectra during the rise to maximum. The nebular spectra of SN 2011dh show a box-shaped emission in the red wing of the [O I] 6300−6363 Å feature, that is attributed to Hα emission from a shock-excited circumstellar material. The analysis of nebular spectra indicates that $\sim$0.2 $M_\odot$ of oxygen was ejected during the explosion. Further, the [Ca II]/[O I] line ratio in the nebular phase is $\sim$0.7, indicating a progenitor with a main-sequence mass of 10–15 $M_\odot$.

Key words: techniques: photometric – techniques: spectroscopic – supernovae: general – supernovae: individual: SN 2011dh.

1 INTRODUCTION

Core-collapse supernovae (CCSNe) result from the violent death of massive stars with initial masses greater than 8 $M_\odot$. Considerable diversity is observed in the photometric and spectroscopic properties of these objects, leading to their classification into various classes. The CCSNe that show the presence of strong hydrogen lines in their spectra close to maximum light are designated as Type II. The hydrogen-deficient CCSNe are designated Type Ib or Type Ic based on the presence, or absence, of helium lines, respectively, at light maximum. A further subclassification of Type II supernovae into Type IIP (long plateau in the light curve) and Type IIL (linear decline after peak brightness) is done based on their light curves. However, there are some transitional events e.g. SN 1987K (Filippenko 1988), SN 1993J (Barbon et al. 1995; Prabhu et al. 1995), SN 2008ax (Pastorello et al. 2008, Chornock et al. 2011), whose spectra at the early phase are dominated by H lines, very similar to the Type II supernovae, but in the later phases, their spectra are dominated by He lines, similar to the Type Ib events. Because of their similarity with Type II supernovae in the early phase and later exhibiting properties of Type Ib supernovae, these transitional objects are classified as Type IIb supernovae (Woosley et al. 1987). The number of supernovae identified as IIb events is limited, although recently these objects gained greater interest as they provide a link between the hydrogen-rich Type II (Type IIP and Type IIL) supernovae and the hydrogen-deficient Type Ib and Ic objects. The Type Ib, Ic and IIb supernovae are collectively known as stripped envelope CCSNe.

There is a growing consensus that the observed diversity in the properties of CCSNe is due to the state of the progenitor star's hydrogen and helium envelopes at the time of explosion (Filippenko 1997; Heger et al. 2003; Gal-Yam et al. 2007). The subclassification of CCSNe can be represented in the form of a sequence – IIP→IIL→IIb→Ib→Ic, and can possibly be interpreted as a sequence of stripping of the H envelope. The progenitors of Type IIP supernovae retain most of the H envelope, while the progenitor stars that lose almost all of the H envelope and retain only a very thin layer of H at the time of explosion produce the type IIb events. The progenitors that have lost their entire hydrogen envelope produce the type Ib and those that have been stripped off hydrogen and most of their helium result in Type Ic supernovae. In fact, detailed modelling of Type IIb supernovae have shown that their observed light curves can be reproduced well using helium stars with a very thin hydrogen envelope (Mazzali et al. 2009).

In a few cases, progenitors of nearby CCSNe have been identified in the high-resolution, pre-explosion images obtained by the *Hubble Space Telescope* (*HST*) and other large facilities. The detected

⋆E-mail: dks@iiap.res.in

progenitors of Type IIP supernovae indicate that they come from red supergiants (e.g. Smartt 2009, and references therein). For the Type IIb supernovae, the situation is not very clear. Massive stars in close binary systems experiencing strong mass transfer (Podsiadlowski et al. 1993), or very massive single stars with strong stellar winds (Heger et al. 2003), are considered as potential progenitors of type IIb events. The progenitor system of SN 1993J was identified as a K0Ia star (Filippenko, Matheson & Ho 1993) in a binary system, with an early B-supergiant companion (Maund & Smartt 2009). Similarly, an interacting binary system, with a slightly later companion star (late B through late F), was suggested as the progenitor of SN 2001ig (Ryder, Murrowood & Stathakis 2006). A source, coinciding with the position of SN 2008ax, was identified in pre-explosion *HST* images (Crockett et al. 2008; Li et al. 2008). However, its interpretation as the progenitor is ambiguous. Crockett et al. (2008) have explored the possibility of (i) the progenitor being a single massive star that lost most of its hydrogen envelope through radiatively driven mass-loss processes, before exploding as a helium-rich Wolf–Rayet star, or (ii) a stripped star in an interacting binary in a low-mass cluster. The [Ca II]/[O I] ratio in nebular spectra of SN 2008ax, however, is more consistent with the low-mass binary scenario (Taubenberger et al. 2011).

A new supernova was discovered by A. Riou on 2011 June 1.893 in the nearby galaxy M51 (Griga et al. 2011). Images of the galaxy obtained on May 31.893 also showed the supernova, but, no object was visible at the position of the supernova in the images of May 30. The Palomar Transient Factory (PTF) independently discovered the supernova on 2011 June 1.19 (Silverman, Filippenko & Cenko 2011), while the PTF observations of May 31.275 do not show the supernova. These observations reduce the uncertainty on the date of explosion to better than 0.6 d (Arcavi et al. 2011b). Based on the earliest spectrum of 2011 June 3, the supernova was classified as a young Type II supernova (Silverman et al. 2011; Yamanaka et al. 2011). Arcavi et al. (2011a) noticed the similarity between the spectrum of SN 2011dh and the type IIb events SN 1993J and SN 2008ax, and suggested SN 2011dh was possibly a type IIb event. Further observations on June 12 and 16 by Marion et al. (2011) in the infra-red showed the presence of He I features consistent with its classification as a type IIb event.

SN 2011dh has been followed extensively in a wide wavelength range, from the radio to the X-rays. It was detected at 86 GHz just three days after its discovery by the Combined Array for Research in Millimeter-wave Astronomy (CARMA) (Horesh et al. 2011) and has been followed with the Very-long-baseline interferometry (VLBI; Marti-Vidal et al. 2011; Bietenholz et al. 2012) and Expanded Very Large Array (EVLA) over the first 100 d of its evolution (Krauss et al. 2012). SN 2011dh was also detected in the X-rays by the *Swift*/X-ray Telescope (*XRT*) ∼3 d after the explosion, and has subsequently been followed with both *Swift* and *Chandra*. A multi-wavelength study of SN 2011dh spanning the radio, millimetre, X-ray and gamma-ray bands during the first few seconds to weeks following the explosion is presented by Soderberg et al. (2012). Maund et al. (2011) have presented the optical photometric and spectroscopic data of SN 2011dh during the first 50 d after explosion, while photometric data covering the first ∼300 d after explosion, with a preliminary light-curve modelling, have been presented by Tsvetkov et al. (2012).

The reddening in the Milky Way in the direction of M51 is $E(B-V)_{\rm gal} = 0.035$ mag (Schlegel, Finkbeiner & Davis 1998). High-resolution spectroscopy of SN 2011dh did not show any narrow lines due to interstellar medium in the host galaxy, except the Na ID doublet due to the interstellar medium in the Milky Way (Arcavi et al. 2011b; Ritchey & Wallerstein 2012; Vinko et al. 2012), indicating low extinction within the host galaxy. Hence, $E(B-V) = 0.035$ mag is adopted as total reddening.

A search for the progenitor star in the archival pre-explosion *HST* images obtained with the Advanced Camera for Survey led to the detection of a luminous star at the position of the supernova (Maund et al. 2011; Murphy et al. 2011; Van Dyk et al. 2011), but its nature and association with the supernova remain controversial. The spectral energy distribution (SED) of this candidate progenitor star was found to be consistent with an F8 supergiant, but with a higher luminosity and a more extended radius than a normal supergiant (Maund et al. 2011; Van Dyk et al. 2011; Vinko et al. 2012). Maund et al. (2011) and Van Dyk et al. (2011) estimate the initial mass of this proposed progenitor to be $M_{\rm ZAMS} \sim 15$–$20\,{\rm M}_{\odot}$. The observed early optical, radio and X-ray observations of SN 2011dh (Arcavi et al. 2011b; Van Dyk et al. 2011; Soderberg et al. 2012) and the re-analyses of the *HST* images with an improved distance to M51 (Vinko et al. 2012) all point towards a compact progenitor, while hydrodynamical modelling suggests that a large progenitor star with radius ∼200 $\rm R_{\odot}$ is required to reproduce the early light curve (Bersten et al. 2012). The association of the yellow supergiant with SN 2011dh needs further exploration. Benvenuto, Bersten & Nomoto (2013) explored the possibility of the existence of such a star in a close binary system by performing binary stellar evolution calculations and arrived at the conclusion that a close binary system of solar composition stars with masses of $16\,{\rm M}_{\odot} + 10\,{\rm M}_{\odot}$ could lead to the evolution of the donor star into a yellow supergiant consistent with the candidate progenitor detected in the *HST* images.

In this paper we present a detailed analysis of optical photometry in *U*, *B*, *V*, *R* and *I* bands and medium-resolution spectroscopy of SN 2011dh during the first one year after the explosion, obtained with the 2-m Himalayan Chandra Telescope (HCT) of the Indian Astronomical Observatory (IAO), Hanle, India.

2 OBSERVATION AND DATA REDUCTION

2.1 Photometry

Photometric monitoring of SN 2011dh was carried out with the 2-m HCT of the IAO, Hanle, India. The imaging observations were made in Bessell's *U*, *B*, *V*, *R* and *I* filters available with the Himalaya Faint Object Spectrograph Camera (HFOSC). HFOSC is equipped with a 2k × 4k pixels, SITe CCD chip. The central 2k × 2k pixels of the chip was used for imaging observations. Plate scale of the telescope-detector system is 0.296 arcsec pixel^{-1} and the central 2k × 2k pixels of the chip cover 10 × 10 arcmin^2 region of the sky.

Photometric monitoring of SN 2011dh started on 2011 June 03 (JD 245 5716.20) and continued till 2012 May 20 (JD 245 6068.36), with a break in between, during 2011 September 06 to 2011 November 19, when the object was in solar conjunction. The object was monitored in *B*, *V*, *R* and *I* bands during the entire period, whereas the observations in *U* band could be obtained only up to 2011 November 19. Photometric standard fields from Landolt's catalogue (Landolt 1992) observed on 2011 June 3, under photometric conditions were used for calibration. Standard fields observed during 2005–2006 as a part of an extensive monitoring campaign of SN 2005cs, also hosted in M51, were also used, together with the observations of 2011 June 3, for photometric calibration of a sequence of secondary standards in the supernova field.

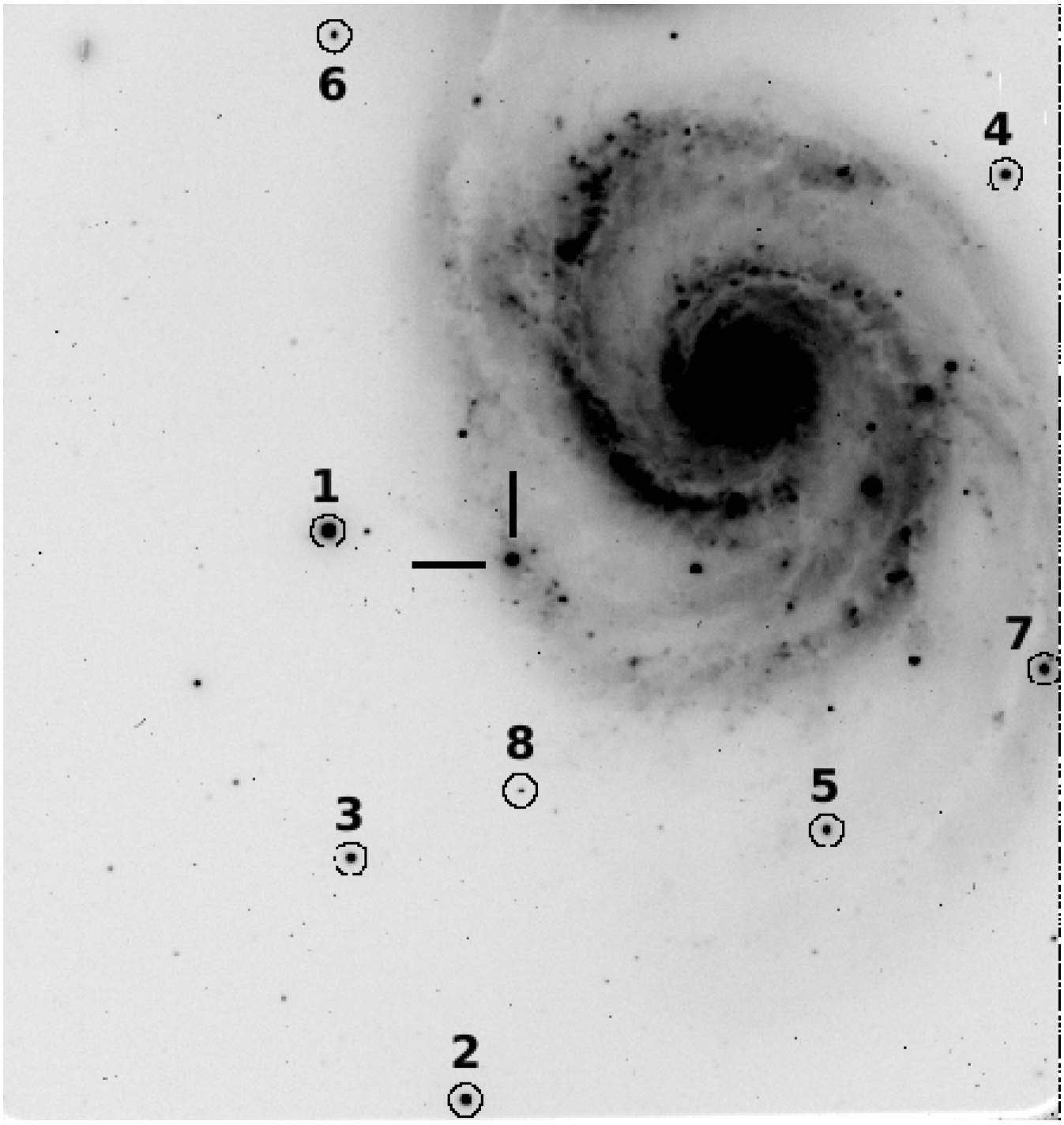

Figure 1. Identification chart for SN 2011dh. The stars used as local standards are marked with numbers 1–8. North is up and east to the left. The field of view is 10×10 arcmin^2.

All the imaging data were pre-processed in the standard way using various tasks available within IRAF.[1] Instrumental magnitudes of the standard stars were obtained using aperture photometry, with an optimal aperture, which is usually three to four times the full width half-maximum (FWHM) of the stellar profile, determined using the aperture growth curve. Aperture correction between the optimal aperture and an aperture close to the FWHM of the stellar profile that had the maximum signal-to-noise ratio was determined using the bright stars in the field and then applied to the fainter ones. Correction for atmospheric extinction was made using the average extinction values for the site (Stalin et al. 2008), and the average colour terms for the system were used to determine the photometric zero-points on individual nights. These were then used to calibrate a sequence of local standards in the supernova field (marked in Fig. 1) observed on the same nights as the standard fields. The U, B, V, R and

[1] IRAF is distributed by the National Optical Astronomy Observatories, which are operated by the Association of Universities for Research in Astronomy, Inc., under cooperative agreement with the National Science Foundation.

Table 1. Magnitudes for the sequence of secondary standard stars in the field of SN 2011dh.

ID	*U*	*B*	*V*	*R*	*I*
1	14.689 ± 0.013	14.339 ± 0.015	13.640 ± 0.023	13.223 ± 0.024	12.899 ± 0.048
2	15.496 ± 0.023	15.473 ± 0.028	14.851 ± 0.027	14.498 ± 0.007	14.100 ± 0.006
3	17.331 ± 0.032	16.561 ± 0.022	15.644 ± 0.028	15.095 ± 0.029	14.636 ± 0.014
4	16.744 ± 0.047	16.216 ± 0.068	15.295 ± 0.090	14.733 ± 0.080	14.153 ± 0.023
5	16.249 ± 0.020	16.221 ± 0.026	15.605 ± 0.030	15.233 ± 0.029	14.866 ± 0.019
6	17.161 ± 0.042	16.974 ± 0.036	16.256 ± 0.003	15.805 ± 0.031	15.371 ± 0.016
7	17.753 ± 0.037	16.586 ± 0.025	15.090 ± 0.027	14.103 ± 0.007	13.058 ± 0.040
8	20.589 ± 0.081	19.429 ± 0.050	17.926 ± 0.037	16.799 ± 0.023	15.540 ± 0.019

I magnitudes of the secondary standards, averaged over four nights, are listed in Table 1. The errors reported with the magnitudes are the standard deviation of the standard magnitudes obtained on the four nights. The magnitudes of the secondary standards obtained using the two separate observing runs, during 2005–2006 and 2011, are in good agreement. Further, we have four secondary standards in common with Pastorello et al. (2009). The average of the absolute value of difference between our magnitudes and those reported by Pastorello et al. (2009) are 0.058, 0.023, 0.030, 0.015 and 0.059 in *U*, *B*, *V*, *R* and *I* bands, respectively.

The supernova is located at the edge of outer spiral arm, 138 arcsec east and 92 arcsec south of the nucleus of M51. During the brighter phase, profile fitting photometry of the supernova is not contaminated much by the underlying galaxy background. However, as the supernova dimmed, profile fitting photometry overestimated the supernova flux, and the photometric precision also degraded. Hence, host galaxy templates in different bands, selected from amongst the best frames of SN 2005cs observations, were used for a more accurate subtraction of the host galaxy background. The magnitudes of the secondary standards in the supernova frames and those of supernova in the template-subtracted frames were obtained using aperture photometry. The night-to-night zero-points were determined using the stars identified as local standards in the supernova field and the supernova magnitudes were calibrated differentially with respect to the local standards. The estimated supernova magnitudes in *U*, *B*, *V*, *R* and *I* bands are listed in Table 2. The errors on the magnitudes were estimated by adding in quadrature the errors associated with nightly photometric zero-points, and the fitting errors as computed by IRAF.

2.2 Spectroscopy

Medium-resolution optical spectra of SN 2011dh were obtained on 20 epochs. The spectra were obtained using grism Gr 7 (wavelength range 3500–7800 Å) and Gr 8 (wavelength range 5200–9250 Å) available with the HFOSC instrument. Our spectroscopic monitoring, which started on JD 245 5716 and continued till JD 245 6072, presents the spectral evolution from ∼3 d to ∼1 year after the explosion. A journal of spectroscopic observation is provided in Table 3. Spectrophotometric standards Feige 34, Feige 110, Hz 44, Wolf 1346 were observed for determining the instrumental response correction.

All spectra were reduced in the standard manner using various tasks available in IRAF. The two-dimensional spectral frames were bias corrected and flat-fielded, and the one-dimensional spectra were extracted using the optimal extraction method (Horne 1986). Arc lamp spectra were used for applying wavelength calibration. The bright night sky emission lines were used to cross check the wavelength calibration, and whenever required, small shifts were applied to the observed spectra. Instrumental response was corrected using the spectra of spectrophotometric standard stars observed during the same night. On some nights, when spectrophotometric standard stars could not be observed, spectra of standard stars observed on nearby nights were used for the correction. The flux calibrated spectra in the blue and red regions were combined after proper scaling to get the final spectrum on a relative flux scale. The spectra were then brought to an absolute flux scale using zero-points determined from broad-band *UBVRI* magnitudes. The supernova spectra were then corrected for the host galaxy redshift $z = 0.002$ and dereddened for a total reddening of $E(B - V) = 0.035$ mag. The telluric lines have not been removed from the spectra due to the absence of a template hot star spectrum with a good signal-to-noise ratio.

3 RESULTS

3.1 Photometric results

3.1.1 Light curves

The light curves of SN 2011dh in *U*, *B*, *V*, *R* and *I* bands are presented in Fig. 2. The observed supernova magnitudes were used to obtain photometric parameters of SN 2011dh in different bands, and are listed in Table 4. The maximum in *B* band occurred on JD 245 5732.60 ± 0.35, at an apparent magnitude of 13.388 ± 0.022. The maximum in *U* band occurred ∼4 d before the *B*-band maximum, whereas the maximum in the *V*, *R* and *I* bands occurred ∼1, 1.5 and 3.3 d, respectively, after *B* maximum. The date of maximum and peak magnitudes in different bands are reported by Tsvetkov et al. (2012). Except for the *U* band, where our estimate of JD maximum differs by ∼1.5 d, our estimates of the date of maximum and peak observed magnitudes are consistent with those of Tsvetkov et al. (2012). A reddening of $E(B - V) = 0.035$ mag, and a distance of 8.4 ± 0.7 Mpc (Vinko et al. 2012) are used in obtaining the peak absolute magnitudes of SN 2011dh. The errors in the absolute magnitudes have been arrived at by using uncertainties in the peak magnitude and the distance modulus of the host galaxy. The rise time to maximum in different bands is also listed in Table 4. The rise time of SN 2011dh in different bands is very similar to that of SN 2008ax (Pastorello et al. 2008; Taubenberger et al. 2011).

Light curves of SN 2011dh are compared with those of Type IIb supernovae 2008ax (Pastorello et al. 2008; Taubenberger et al. 2011), 1993J (Lewis et al. 1994; Barbon et al. 1995), 1996cb (Qui et al. 1999) and the Type Ib SN 1999ex (Stritzinger et al. 2002) in Figs 3 and 4. Fig. 3 shows the evolution of the light curves during the first 100 d after explosion and Fig. 4 shows the light-curve evolution beyond 100 d after explosion. The observed magnitudes of the supernovae have been normalized to their respective peak magnitudes and shifted in time to the epoch of maximum brightness in *B* band. The light curves of SN 2011dh in the *B* and *V* bands are

Table 2. Photometric observations of SN 2011dh.

Date	JD	Phase[a] (d)	*U*	*B*	*V*	*R*	*I*
03/06/2011	245 5716.20	3.20	15.051 ± 0.024	15.379 ± 0.014	14.924 ± 0.016	14.576 ± 0.019	14.461 ± 0.014
05/06/2011	245 5718.22	5.22	14.821 ± 0.013	14.972 ± 0.004	14.407 ± 0.025	14.025 ± 0.017	14.054 ± 0.023
06/06/2011	245 5719.22	6.22	14.528 ± 0.020	14.666 ± 0.010	14.074 ± 0.018	13.738 ± 0.020	13.787 ± 0.019
07/06/2011	245 5720.22	7.22			13.862 ± 0.014	13.459 ± 0.010	13.513 ± 0.025
14/06/2011	245 5727.32	14.32	13.620 ± 0.013	13.632 ± 0.010	12.867 ± 0.014	12.577 ± 0.026	12.530 ± 0.017
19/06/2011	245 5732.28	19.28	13.694 ± 0.026	13.389 ± 0.012	12.624 ± 0.020	12.294 ± 0.009	12.253 ± 0.019
20/06/2011	245 5733.23	20.33		13.394 ± 0.013	12.608 ± 0.017	12.363 ± 0.034	12.250 ± 0.192
27/06/2011	245 5740.28	27.28	14.561 ± 0.022	14.167 ± 0.027	12.960 ± 0.025	12.445 ± 0.014	12.256 ± 0.032
11/07/2011	245 5754.21	41.21	16.133 ± 0.022	15.442 ± 0.031	13.897 ± 0.037	13.161 ± 0.011	12.795 ± 0.022
16/07/2011	245 5759.23	46.23	16.326 ± 0.031	15.582 ± 0.024	14.044 ± 0.016	13.303 ± 0.029	12.947 ± 0.014
17/07/2011	245 5760.21	47.21	16.321 ± 0.016	15.570 ± 0.035	14.089 ± 0.022	13.336 ± 0.036	12.971 ± 0.018
18/07/2011	245 5761.23	48.23	16.354 ± 0.014	15.624 ± 0.029	14.101 ± 0.016	13.333 ± 0.041	12.984 ± 0.014
20/07/2011	245 5763.18	50.18		15.583 ± 0.009	14.135 ± 0.013	13.413 ± 0.024	13.062 ± 0.013
27/07/2011	245 5770.18	57.18	16.320 ± 0.018	15.685 ± 0.007	14.319 ± 0.024	13.590 ± 0.027	13.213 ± 0.018
02/08/2011	245 5776.20	63.20		15.723 ± 0.010	14.421 ± 0.019	13.685 ± 0.021	13.292 ± 0.019
11/08/2011	245 5785.13	72.13			14.574 ± 0.032	13.900 ± 0.019	13.468 ± 0.012
18/08/2011	245 5792.13	79.13		15.842 ± 0.012	14.673 ± 0.027	14.039 ± 0.016	13.594 ± 0.013
29/08/2011	245 5803.14	90.14			14.907 ± 0.018	14.268 ± 0.017	13.820 ± 0.018
06/09/2011	245 5811.09	98.09	16.560 ± 0.024	16.135 ± 0.014	15.038 ± 0.030	14.478 ± 0.007	13.979 ± 0.018
19/11/2011	245 5885.50	172.50	17.804 ± 0.055	17.427 ± 0.033	16.784 ± 0.032	16.105 ± 0.021	15.784 ± 0.024
24/11/2011	245 5889.51	176.51		17.534 ± 0.032	16.898 ± 0.027	16.265 ± 0.044	
30/11/2011	245 5896.48	183.48		17.673 ± 0.023	17.053 ± 0.026	16.348 ± 0.017	16.084 ± 0.058
12/12/2011	245 5907.52	194.52			17.297 ± 0.024	16.540 ± 0.020	
13/12/2011	245 5908.53	195.53			17.284 ± 0.035	16.572 ± 0.021	
23/12/2011	245 5919.43	206.43		18.085 ± 0.020	17.478 ± 0.021	16.734 ± 0.024	16.510 ± 0.057
28/12/2011	245 5924.47	211.47		18.147 ± 0.022	17.506 ± 0.039	16.862 ± 0.018	16.624 ± 0.035
04/01/2012	245 5931.40	218.40		18.357 ± 0.044	17.786 ± 0.039	16.945 ± 0.033	16.731 ± 0.034
10/01/2012	245 5937.48	224.48			17.913 ± 0.041	17.043 ± 0.023	16.871 ± 0.025
14/01/2012	245 5941.49	228.49		18.416 ± 0.031	17.921 ± 0.021	17.048 ± 0.032	
18/01/2012	245 5944.51	231.51		18.553 ± 0.018	17.959 ± 0.028	17.204 ± 0.019	16.986 ± 0.029
28/01/2012	245 5955.47	242.47		18.766 ± 0.036	18.281 ± 0.015	17.375 ± 0.025	17.178 ± 0.023
26/02/2012	245 5984.34	271.34		18.974 ± 0.034	18.557 ± 0.040	17.666 ± 0.019	17.714 ± 0.080
05/03/2012	245 5992.28	279.28			18.753 ± 0.052	17.775 ± 0.029	
15/03/2012	245 6002.47	289.47			19.052 ± 0.028	18.044 ± 0.022	18.018 ± 0.033
03/04/2012	245 6021.41	308.41		19.839 ± 0.033	19.406 ± 0.027	18.337 ± 0.048	18.181 ± 0.060
13/04/2012	245 6031.31	318.31			19.326 ± 0.058	18.354 ± 0.034	18.287 ± 0.040
08/05/2012	245 6056.29	343.29			19.890 ± 0.047	18.765 ± 0.038	18.812 ± 0.078
20/05/2012	245 6068.36	355.36		20.632 ± 0.088	20.360 ± 0.044	18.933 ± 0.041	19.025 ± 0.070

[a]Observed phase with respect to the date of explosion (JD 245 5713.0).

very similar to those of SNe 2008ax, 1999ex and 1993J. The decline in magnitude within 15 d from the date of maximum (Δm_{15}), for the *B*, *V*, *R* and *I* bands is estimated to be $\Delta m_{15}(B) = 1.75 \pm 0.18$, $\Delta m_{15}(V) = 0.98 \pm 0.04$, $\Delta m_{15}(R) = 0.64 \pm 0.03$ and $\Delta m_{15}(I) = 0.47 \pm 0.01$. Tsvetkov et al. (2012) estimate $\Delta m_{15}(B) = 1.64$ mag, which is consistent with our estimate. These values are marginally larger than the Δm_{15} values of SN 2008ax reported by Taubenberger et al. (2011), but similar to the Δm_{15} values of SN 1993J in the *B* and *V* bands.

The slope of the light curve in the *B*, *V*, *R* and *I* bands during ∼60–100 is estimated to be 1.09 ± 0.15, 1.76 ± 0.04, 2.16 ± 0.05 and 1.90 ± 0.05 mag $(100\,\mathrm{d})^{-1}$, respectively. A change in the slope is noticed in all the bands during days ∼170–360. The *B* and *V* light curves show a steepening, with the slope being 1.71 ± 0.13 mag $(100\,\mathrm{d})^{-1}$ in the *B* and 1.83 ± 0.11 mag $(100\,\mathrm{d})^{-1}$ in the *V*. On the other hand, the *R* and *I* light curves show a flattening with the slope being 1.51 ± 0.05 mag $(100\,\mathrm{d})^{-1}$ in *R* and 1.70 ± 0.06 mag $(100\,\mathrm{d})^{-1}$ in *I*. The steepening of the *B* and *V* light curves could be an indication of early dust formation.

A comparison of late time decline rate of SN 2011dh with that of SN 2008ax shows that except for the *I* band, in which SN 2008ax declines faster, the late phase decline rates of SN 2011dh and SN 2008ax are very close (Taubenberger et al. 2011). Using the available data of SN 1993J, the late phase decline rate, during 100–300 d past explosion, is estimated as 1.39, 1.71, 1.49 and 1.87 mag $(100\,\mathrm{d})^{-1}$ in *B*, *V*, *R* and *I* bands, respectively. This indicates SN 2011dh declines faster than SN 1993J (see also Fig. 4).

3.1.2 Colour curves

The colour curves of SN 2011dh along with supernovae 2008ax, 1996cb, 1993J and 1999ex have been plotted in Fig. 5. The colour curves of SNe 2011dh, 2008ax, 1996cb, 1993J and 1999ex have been corrected for $E(B-V)$ of 0.035, 0.4, 0.12, 0.18 and 0.30, respectively. It is evident from Fig. 5 that the reddening corrected $(B-V)$ and $(V-R)$ colours of SN 2011dh are always redder as compared to the other stripped envelope CCSNe used in comparison. A similar trend is seen in the $(R-I)$ colour also, though not very significant. An additional reddening $E(B-V)$ of ∼0.35 is required to bring the $(B-V)$ and $(V-R)$ colours of SN 2011dh close to those of other supernovae. High-resolution spectroscopy of SN 2011dh does not

Table 3. Log of spectroscopic observations of SN 2011dh.

Date	JD 245 0000+	Phase[a] (d)	Range (Å)
03/06/2011	245 5716.29	3.29	3500–7000;5200–9100
06/06/2011	245 5719.18	6.18	3500–7000;5200–9100
19/06/2011	245 5732.29	19.29	3500–7000;5200–9100
20/06/2011	245 5733.24	20.24	3500–7000;5200–9100
27/06/2011	245 5740.29	27.29	3500–7000;5200–9100
11/07/2011	245 5754.22	41.22	3500–7000;5200–9100
17/07/2011	245 5760.23	47.23	3500–7000;5200–9100
26/07/2011	245 5769.11	56.11	3500–7000;5200–9100
02/08/2011	245 5776.21	63.21	3500–7000;5200–9100
07/09/2011	245 5812.08	99.08	3500–7000;5200–9100
20/11/2011	245 5886.48	173.48	3500–7000;5200–9100
12/12/2011	245 5908.48	195.48	3500–7000;5200–9100
28/12/2011	245 5923.51	210.51	3500–7000;5200–9100
07/01/2012	245 5934.31	221.31	3500–7000;5200–9100
10/01/2012	245 5937.34	224.34	3500–7000;5200–9100
28/01/2012	245 5955.44	242.44	3500–7000
26/02/2012	245 5984.39	271.39	3500–7000;5200–9100
05/03/2012	245 5992.34	279.34	3500–7000;5200–9100
08/05/2012	245 6056.37	343.37	3500–7000;5200–9100
24/05/2012	245 6072.18	359.18	3500–7000;5200–9100

[a]Observed phase with respect to the date of explosion (JD 245 5713.0).

reveal the presence of any absorbing system within the host galaxy, implying insignificant reddening within the host galaxy. The other possibility is that supernova SN 2011dh is intrinsically redder. A blackbody fit to the spectrum obtained ∼3 d after explosion gives a temperature of ∼7600 K (Arcavi et al. 2011b), which is lower than that expected, at similar epochs, from the explosion of a Red Super Giant. Arcavi et al. (2011b) have argued that the sharp decline in the *g*-band light curve during the first two days after explosion also needs a much lower temperature. It thus appears that the observed redder colour of SN 2011dh is due to its lower temperature and not because of excess reddening within the host galaxy.

3.1.3 Absolute magnitude, bolometric light curve and mass of ^{56}Ni

The *V*-band peak absolute magnitudes of SN 2011dh estimated adopting reddening $E(B-V) = 0.035$ mag and distance 8.4 ± 0.7 Mpc (Vinko et al. 2012) is -17.123 ± 0.18 mag. The peak absolute magnitude of SN 2011dh is ∼1 mag fainter than the mean peak absolute magnitudes of the entire sample of stripped-envelope CCSNe and is ∼0.3 mag fainter than the type IIb sample (Richardson, Branch & Baron 2006). It is fainter than the absolute peak *V* magnitude of some other well-studied Type IIb supernovae SN 1993J (-17.57 ± 0.24; Maund et al. 2004), SN 2003bg (-17.50; Hamuy et al. 2009; Mazzali et al. 2009), SN 2008ax (-17.617 ± 0.43; Taubenberger et al. 2011), SN 2009mg (-17.68 ± 0.48; Oates et al. 2012) and SN 2011fu (-18.50 ± 0.24; Kumar et al. 2013). On the other hand, the absolute peak *V*-band magnitude of SN 2011dh is brighter than SN 1996cb (-16.22; Qui et al. 1999), SN 2007Y (-16.45 ± 0.6; Stritzinger et al. 2009) and SN 2011ei (∼−16; Milisavljevic et al. 2012). It shows that Type IIb supernovae represent an inhomogeneous class in terms of peak *V*-band magnitude, with a wide spread, of more than 2 mag. The absolute *V*-band light curve of SN 2011dh is plotted along with some well-studied stripped

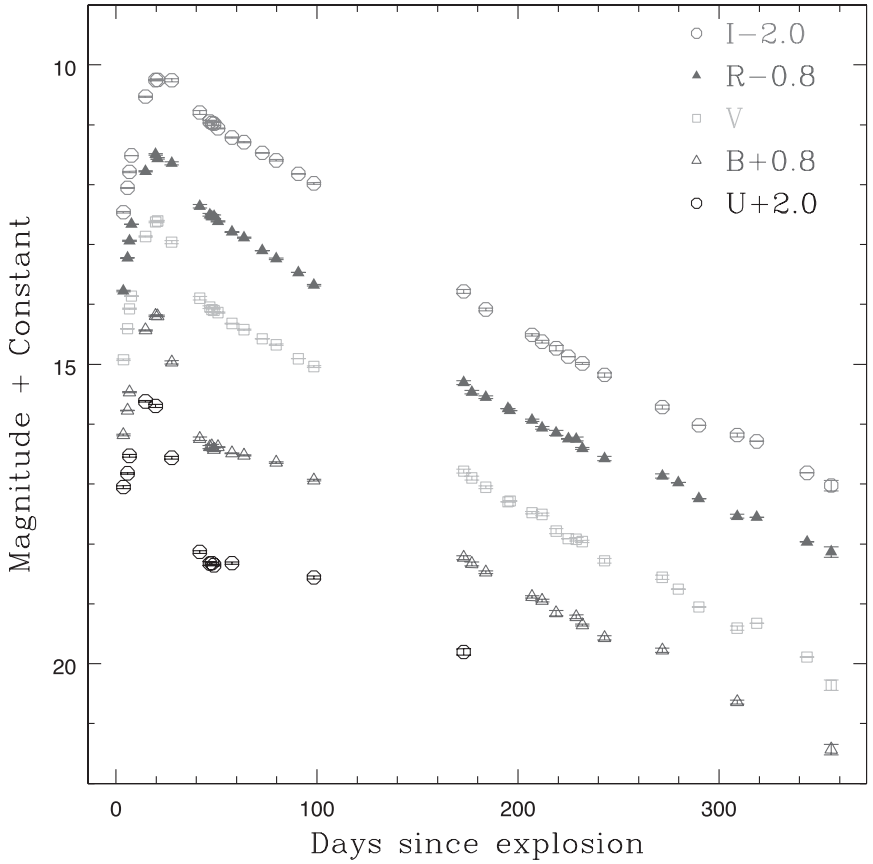

Figure 2. *UBVRI* light curves of SN 2011dh. The light curves have been shifted by the amount indicated in the legend.

Table 4. Photometric parameters.

Band	JD (Max)	Peak obs. mag	Peak abs. mag	Rise time (d)
U	245 5728.82 ± 0.43	13.605 ± 0.037	−16.186 ± 0.18	15.8 ± 0.5
B	245 5732.60 ± 0.35	13.388 ± 0.022	−16.378 ± 0.18	19.6 ± 0.5
V	245 5733.57 ± 0.28	12.607 ± 0.016	−17.123 ± 0.18	20.6 ± 0.5
R	245 5734.11 ± 0.20	12.270 ± 0.032	−17.433 ± 0.18	21.3 ± 0.5
I	245 5735.92 ± 0.31	12.196 ± 0.035	−17.477 ± 0.18	22.9 ± 0.5

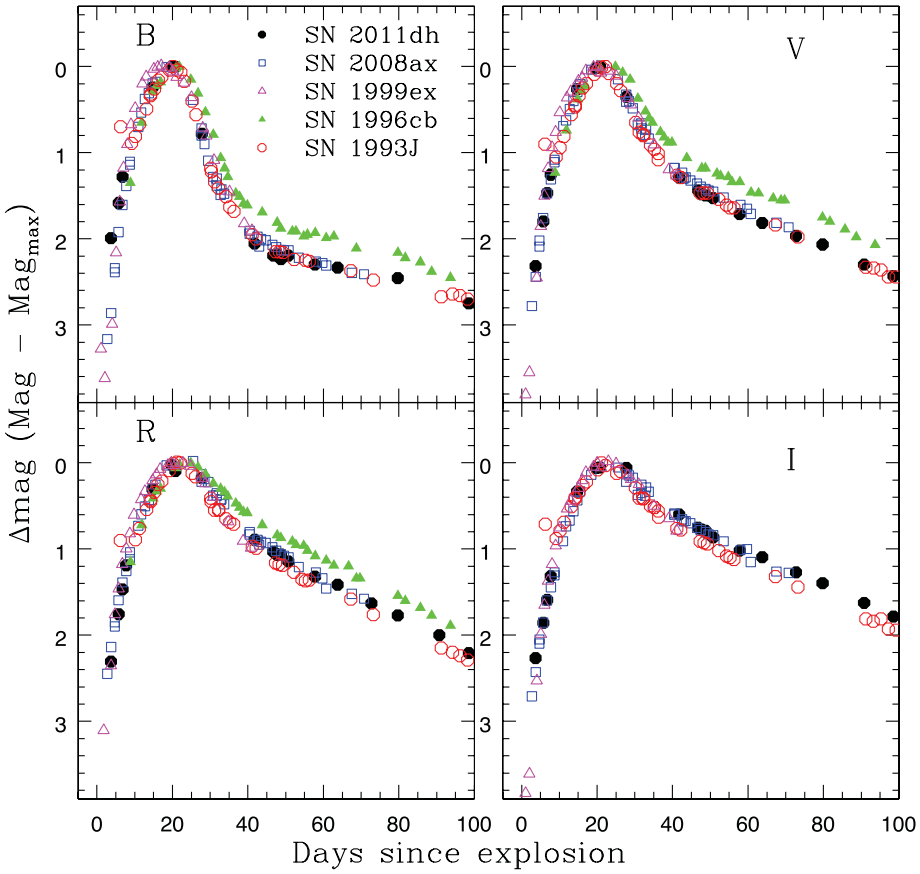

Figure 3. Comparison of *UBVRI* light curves of SN 2011dh with those of SN 2008ax, SN 1999ex, SN 1996cb and SN 1993J, during the early phase. The light curves have been normalized as described in the text.

envelope CCSNe in Fig. 6. The light curves indicate that SN 2011dh declines at a rate of 1.83 mag $(100\,\mathrm{d})^{-1}$ during days 172–353, while SN 2008ax declines at a rate of 1.66 mag $(100\,\mathrm{d})^{-1}$ during days 144–353, and SN 1993J declines at a rate of 1.46 mag $(100\,\mathrm{d})^{-1}$ during days 181–340. It appears that, in general, the light curves of Type IIb SNe decline with a rate faster than the decline rate expected from the decay of $^{56}\mathrm{Co}\rightarrow{}^{56}\mathrm{Fe}$ [0.98 mag $(100\,\mathrm{d})^{-1}$], indicating the γ-rays produced in the decay may not be completely trapped by the supernova ejecta.

Quasi-bolometric light curve of SN 2011dh is obtained using the observed *UBVRI* magnitudes corrected for reddening, and converted to their respective monochromatic flux using the zero-points provided by Bessell, Castelli & Plez (1998). The bolometric fluxes are derived by fitting a spline curve to the *U*, *B*, *V*, *R* and *I* fluxes and integrating over the wavelength range 3100 Å to 10600 Å determined by the response of the filters used for observations. We have observations in the *U* band till November 19, and hence the contribution from *U* band is included in the bolometric light curve till November 19 only. There are a few nights when we do not have observations in either the *U*, *B* or *I* bands. For estimating bolometric flux, the magnitudes of the missing bands, on these nights, were estimated by interpolating the observed magnitudes of the neighbouring nights. The quasi-bolometric light curve of SN 2011dh along with the bolometric light curves of Type IIb SN 2008ax and SN 1993J is plotted in Fig. 7. The quasi-bolometric light curves of SN 2008ax are constructed using the published *U*, *B*, *V*, *R* and *I* magnitudes (Pastorello et al. 2008; Taubenberger et al. 2011) in a manner similar to SN 2011dh. The bolometric light curve of SN 1993J was taken from Lewis et al. (1994), which includes optical and NIR data. The total reddening for SN 2008ax is taken as $E(B-V) = 0.4$ mag (Taubenberger et al. 2011) and distance of 9.6 Mpc (Pastorello et al. 2008) is used. The rise to maximum and subsequent evolution of the quasi-bolometric light curve of SN 2011dh is similar to the other Type IIb supernovae in comparison. However, SN 2011dh is fainter than both SN 2008ax and SN 1993J.

The mass of ^{56}Ni required to power the quasi-bolometric light curve can be estimated using Arnett's rule (Arnett 1982). Under the assumption that the radioactivity powers the light curve and

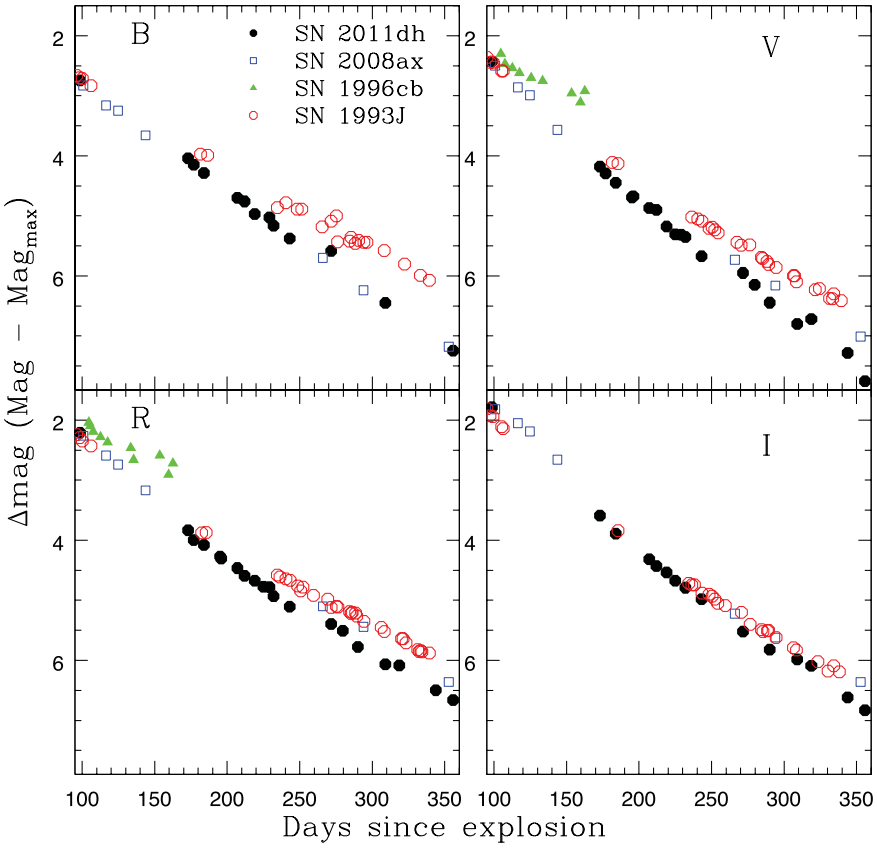

Figure 4. Comparison of *UBVRI* light curves of SN 2011dh with those of SN 2008ax, SN 1996cb and SN 1993J, during the late phase. The light curves have been normalized as described in the text.

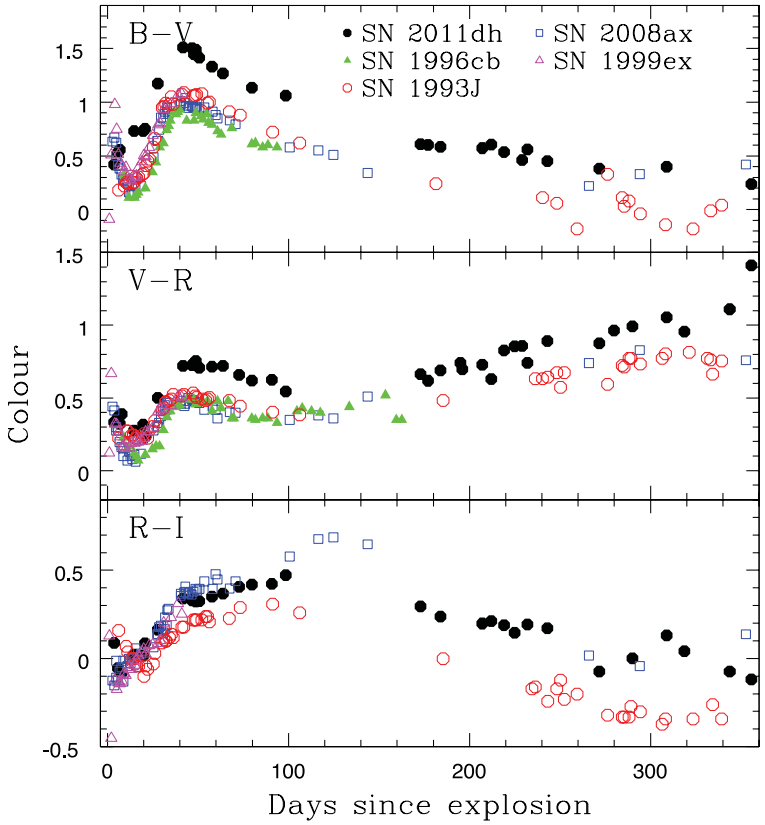

Figure 5. Comparison of colour curves of SN 2011dh with those of SN 2008ax, SN 1999ex, SN 1996cb and SN 1993J.

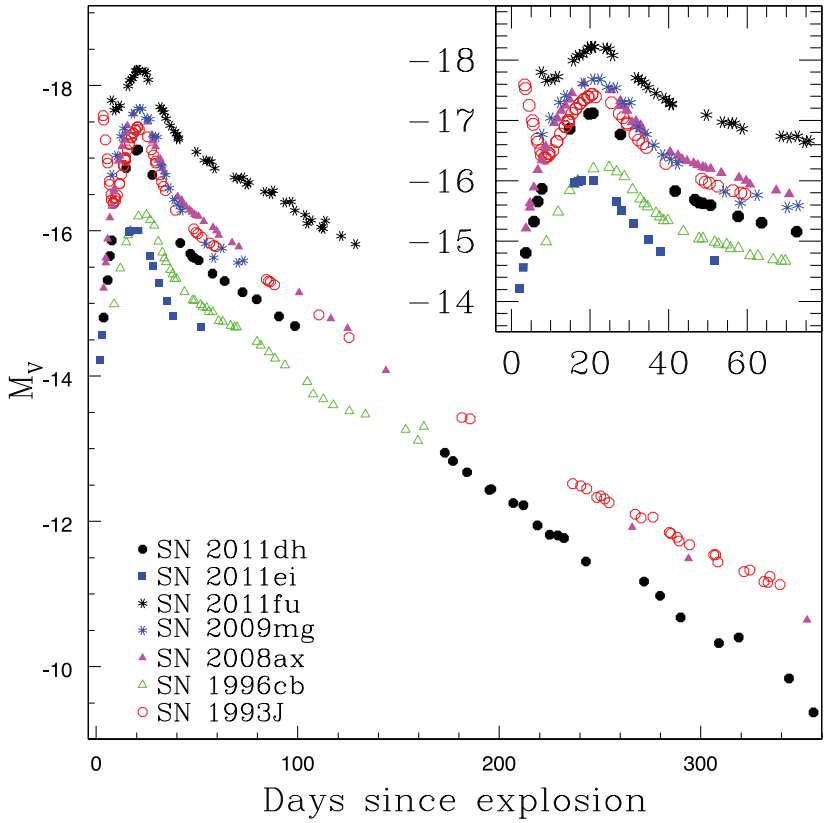

Figure 6. Comparison of the absolute *V* light curve of SN 2011dh with those of SN 2011fu, SN 2011ei, SN 2009mg, SN 2008ax, SN 1996cb and SN 1993J. Inset shows the early evolution of the light curve.

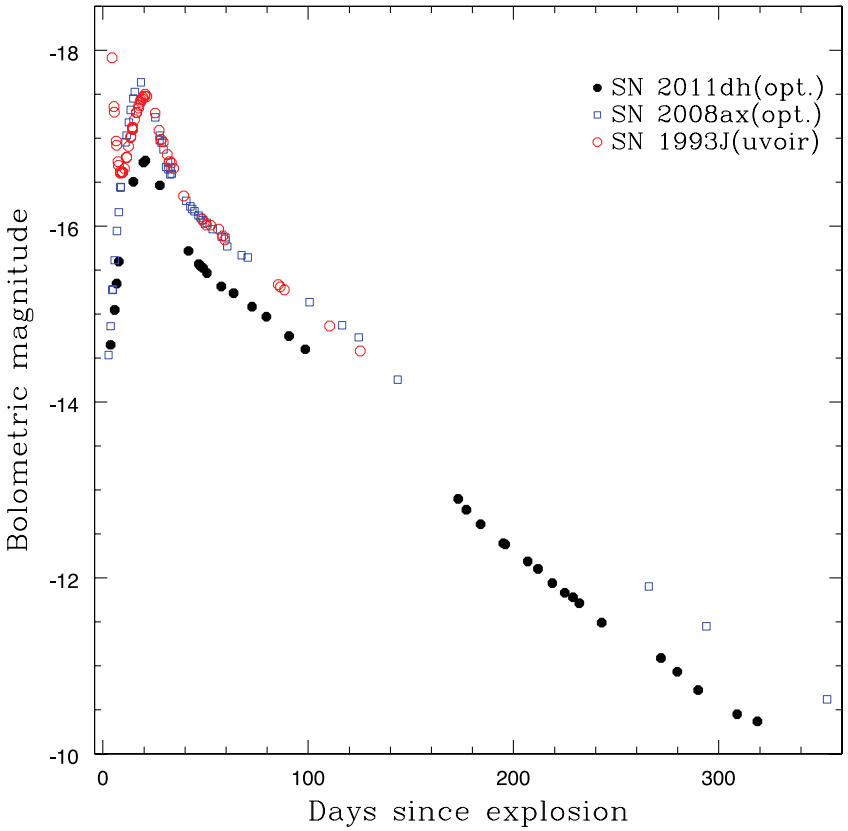

Figure 7. Quasi-bolometric light curve of SN 2011dh. Also plotted in the figure, for comparison, are the bolometric light curves of SN 1993J and SN 2008ax.

at maximum light, most of the energy released by radioactivity is still being trapped and thermalized, the peak radiated luminosity is comparable to instantaneous rate of energy release of radioactive decay of ^{56}Ni synthesized during the explosion. The simplified form of Arnett's rule is expressed as

$$M_{Ni} = L_{\rm bol}/\alpha S(t_R), \quad (1)$$

where α is the ratio of bolometric to radioactivity luminosity (near unity) and S is the radioactivity luminosity per unit nickel mass, evaluated at rise time t_R (Nugent et al. 1995). In the case of SN 2011dh, the explosion date has been well constrained to better than 0.6 d between the first detection on May 31.893 and last non-detection on May 31.275 (Arcavi et al. 2011b). The date of explosion can be taken as a mean of these two dates. The photometry reported in Section 3.1.1 and Table 4 shows that the supernova reached maximum in B band on JD 245 5732.60, with B-band rise time of ∼19.6 d. The peak bolometric luminosity of SN 2011dh, estimated using the observed *UBVRI* flux, is 1.267×10^{42} erg s^{-1}. Taking the B-band rise time of SN 2011dh as 19.6 d, mass of ^{56}Ni synthesized in the explosion is estimated to be $0.063 \pm 0.011\,{\rm M}_{\odot}$.

The mass of ^{56}Ni synthesized during the explosion can also be estimated by fitting the energy deposition rate via the ^{56}Ni→^{56}Co→^{56}Fe chain, to the early post-maximum observed bolometric light curve. The energy deposition rate for different values of ^{56}Ni via the ^{56}Ni→^{56}Co→^{56}Fe chain is estimated using the analytical formula by Nadyozhin (1994). It is found that the energy deposition rate corresponding to mass of ^{56}Ni as $0.070\,{\rm M}_{\odot}$ fits the early post-maximum decline of the observed quasi-bolometric light curve of SN 2011dh.

Vinko et al. (2004) provide a simple analytic model to fit the observed bolometric light curve of supernovae. This model takes into account the energy deposition due to γ-rays produced in the decay chain ^{56}Ni→^{56}Co→^{56}Fe and due to positrons. We fit the early post-maximum decline phase (<30 d after maximum) of the observed bolometric light curve following the formulation by Vinko et al., to estimate the mass of ^{56}Ni. For the total ejected mass of ∼2 $\,{\rm M}_{\odot}$ (Bersten et al. 2012) and the expansion velocity of the ejecta as inferred from Fe II lines, the optical depth for γ-rays and positrons during the early post-maximum decline phase is found to be high and the probability of γ-rays and positrons to escape from the ejecta is very low. Under the assumption that the diffusion time is short, mass of ^{56}Ni is estimated by approximating the energy emitted per second (i.e. bolometric luminosity) to the rate of the energy deposition at different times. A ^{56}Ni mass of $0.067 \pm 0.013\,{\rm M}_{\odot}$ is found to fit the early post-maximum decline of the quasi-bolometric light curve.

The light curve of supernovae at late phases is powered by the ^{56}Co→^{56}Fe decay. If all the γ-rays produced by the decay are trapped in the supernova ejecta, the exponential tail of the bolometric light curve during the nebular phase can also be used to constrain the mass of ^{56}Ni produced in the explosion (Hamuy 2003). The slope of the bolometric light curve of SN 2011dh during days 60 to 100 is 1.79 mag (100 d)$^{-1}$, which is faster compared to the expected decay rate of ^{56}Co→^{56}Fe [0.98 mag (100 d)$^{-1}$]. However, the observed slope can be used to estimate a lower limit of the mass of ^{56}Ni. Using the bolometric flux during days 60 to 98 we calculate the lower limit of ^{56}Ni mass as $0.037 \pm 0.004\,{\rm M}_{\odot}$.

It is to be noted here that while calculating the bolometric light curve of SN 2011dh, contribution due to missing bands in ultraviolet and infra-red has not been taken into account. In the case of SN 1993J Wada & Uneo (1997) have shown that before the second maximum, the flux emitted in J band was ∼8 per cent of the total flux from U to J band, and was ∼15 per cent after the second maximum. The blackbody fit to the photometric data shows that the photospheric temperature of SN 1993J close to maximum light was ∼8200 K (Lewis et al. 1994). Richmond et al. (1994) have estimated the fraction of total blackbody flux emitted in the *UBVRI* bands and shown it to be ∼70 per cent at a blackbody temperature of ∼8000 K. For SN 2008ax, the UV contribution to the pseudo-bolometric light curve is always less than ∼15 per cent, and at the time of maximum it is less than ∼10 per cent (Taubenberger et al. 2011). In a recent paper, Marion et al. (2013) show that in the case of SN 2011dh the NIR contribution at peak is ∼35 per cent, and increases to ∼52 per cent by day 34. After accounting for the missing NIR band flux, the peak bolometric flux of SN 2011dh is 1.711×10^{42} erg sec^{-1} and the mass of ^{56}Ni is $0.084\,{\rm M}_{\odot}$. The inclusion of missing NIR flux to quasi-bolometric flux leads to ^{56}Ni mass of $0.095\,{\rm M}_{\odot}$ and $0.091\,{\rm M}_{\odot}$, using Nadyozhin (1994) and Vinko et al. (2004) formulation, respectively.

3.2 Spectroscopic results

3.2.1 Pre-maximum spectral evolution

The pre-maximum spectra of SN 2011dh obtained ∼3 and 6 d after explosion are shown in Fig. 8. The spectrum of day 3 shows a blue continuum that drops below ∼5000 Å. The prominent noticeable features in the first spectrum are the broad P-Cygni absorption of Hα and absorptions due to Hβ and Hγ, Ca II H&K and NIR triplet. To identify the other features seen in the spectrum, the observed spectrum is compared with the synthetic spectrum generated using SYN++.

SYN++ is a rewrite of the parametrized spectrum synthesis code SYNOW, with a new structured input control file format and with more complete atomic data files (Thomas, Nugent & Meza 2011). The basic assumption of SYNOW includes spherically symmetric and homologously expanding ejecta ($v \propto r$), local thermodynamic equilibrium (LTE) for level populations and resonant scattering line formation above a sharp photosphere emitting a blackbody continuum. The line formation is treated using the Sobolev approximation (Sobolev 1957; Jeffery & Branch 1990). The optical depth τ of the strongest line is a free fitting parameter and optical depths of other lines of the same ion are determined assuming Boltzmann equilibrium at excitation temperature $T_{\rm exc}$. A detailed description of SYNOW has been presented in Fisher (2000) and Branch et al. (2002).

The synthetic spectra for days 3 and 6 are plotted with the observed spectra in Fig. 8. The main species required to produce the observed features have been marked. The synthetic spectrum of day 3 has a blackbody continuum temperature $T_{\rm bb} = 7500$ K, similar to Arcavi et al. (2011b), and photospheric velocity $v_{\rm ph} = 12\,000$ km s^{-1}. The hydrogen line is detached from the photosphere with a minimum velocity $v_{\rm min} = 15\,000$ km s^{-1}. All other lines are undetached. The Hβ and Hγ absorptions are fit reasonably well with $v_{\rm min} = 15\,000$ km s^{-1} and $v_{\rm max} = 23\,000$ km s^{-1}. However, it is difficult to fit the broad absorption of Hα probably due to the LTE and resonance scattering assumptions of SYN++, or due to blend of Hα with other features. Barbon et al. (1995) in their study of SN 1993J attribute the broadness of the Hα absorption to a blend of Hα with Fe II lines, while Elmhamdi et al. (2006) suggest it to be a combination of Hα and Si II in the case of SN 2000H. The broad Hα profile, on the other hand, is interpreted as due to two components of hydrogen with different velocities in the case of SN 2011ei by Milisavljevic et al. (2012). We have explored the possibility of two components of hydrogen to fit the broad Hα absorption, and find

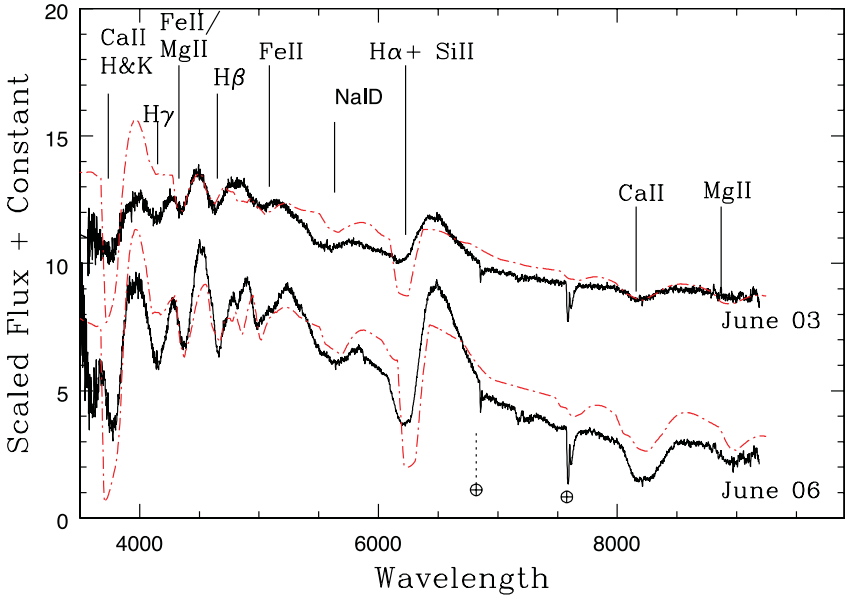

Figure 8. Pre-maximum spectral evolution of SN 2011dh during ∼3 to ∼6 d after explosion. The observed spectra (black, continuous) have been plotted with the synthetic spectra (red, dash–dotted) created using SYN++.

that it does not fit well. A combination of Hα and Si II also does not fit this feature well (see Fig. 8), indicating the requirement of a more detailed modelling. The prominent absorption feature seen at ∼5500 Å is usually attributed to He I 5876 Å and Na ID 5890, 5896 Å lines (Pastorello et al. 2008; Milisavljevic et al. 2012). Since we do not find signature of other lines due to He I, the absorption is most likely due to Na ID alone.

The spectrum of day 6 (June 6) is very similar to the first spectrum. The absorption lines have become sharper and stronger. A synthetic spectrum, with a photospheric temperature $T_{\rm bb} = 6500$ K and photospheric velocity $v_{\rm ph} = 10\,000\,{\rm km\,s^{-1}}$, matches the observed spectrum well. In this case also, hydrogen line is detached from the photosphere with a minimum velocity $v_{\rm min} = 12\,000\,{\rm km\,s^{-1}}$. The same species used to produce the synthetic spectrum corresponding to the day 3 spectrum have been used.

3.2.2 *Early post-maximum spectral evolution*

We had a big gap in spectral monitoring and our next spectrum could be obtained only on 2011 June 19, corresponding to the maximum in *B* band, ∼19.3 d after the explosion. This spectrum together with two other spectra of nearby epochs have been shown in Fig. 9. In the spectrum of June 19, a notch is seen in the emission component of Hα, giving it a double peaked appearance. This is due to the emergence of the He I 6678 Å feature. The P-Cygni features from other He I lines 5876 Å and 7065 Å are clearly identified in this spectrum. The expansion velocity of Hα is $\sim$12800 km s^{-1} and that of He I 5876 Å is $\sim$7300 km s^{-1}. The spectrum indicates the supernova has already entered into a phase wherein the lines due to He I become prominent. The onset of this phase occurred sometime between June 6 and June 19. Marion et al. (2011) have reported non-detection of helium lines in the NIR spectrum of SN 2011dh obtained on June 8, weak evidence of helium in the spectrum obtained on June 12 and an unambiguous detection of helium lines at 10800 Å and 20581 Å in the spectrum obtained on June 16. Weak evidence of He I 5876 Å and 6678 Å lines was also indicated by them in the optical spectrum of June 12, while these lines were clearly seen in their spectrum obtained on June 14. Thus, the He I lines developed in the spectrum of SN 2011dh ∼13 d after the explosion. This is similar to SN 2008ax, in which the He I lines are found to emerge in the NIR spectra at ∼11 d after explosion (Taubenberger et al. 2011).

The next two spectra obtained on June 20 and June 27 are very similar to that of June 19. The He I lines become stronger. In the spectrum of June 27, [O I] 5577 Å line starts appearing.

The spectra of June 19 and June 27 were modelled with the SYN++ code. The synthetic spectra have been plotted with the observed spectra in Fig. 9. The spectrum of June 19 is computed with $T_{\rm bb} = 6500$ K and $v_{\rm ph} = 7000\,{\rm km\,s^{-1}}$, while that of June 27 is computed with $T_{\rm bb} = 4800$ K and $v_{\rm ph} = 6300\,{\rm km\,s^{-1}}$. The main features have been identified and are marked in the figure. Hydrogen and He both are detached from the photosphere with $v_{\rm min}$ of 10 000 km s^{-1} and 7500 km s^{-1}, respectively. The broad absorption of Hα is still not well reproduced; however, Si II helps to improve the fit. Hβ line is fitted well; Hγ gets blended with Fe II lines. Other narrow Fe II lines are well reproduced. Introduction of Sc II (lines at 5527 Å and 5661 Å) is required to produce the two weak troughs bluewards of He I 5876 Å absorption. In the red region of the spectrum, lines due to O I, Mg II and Ca II are well reproduced.

Fig. 10 shows the spectrum of SN 2011dh close to *B* maximum, together with the spectra of other Type IIb supernovae (obtained from SUSPECT archive) at a similar epoch. The lines due to helium are seen in the spectrum of all the supernovae, although with varying strength. The He I 5876 Å line is well developed in all the supernovae. He I 6678 Å has just started appearing in SN 2011dh and SN 1993J; it is stronger in SN 2008ax, while it is not seen in the spectrum of SN 2003bg and SN 2001ig. There is a strong similarity between spectra of SN 2011dh and SN 1993J; the strengths of Hα and He I 5876 Å are similar in both the objects. SN 2011dh has the strongest Ca II NIR feature. At ∼30 d after explosion, the strengths of Hα and the He I 5876 Å line were comparable in the spectrum of SN 2008ax (Pastorello et al. 2008), while, Hα is found to be stronger than He I 5876 in the spectrum of SN 2011dh at ∼27 d after explosion.

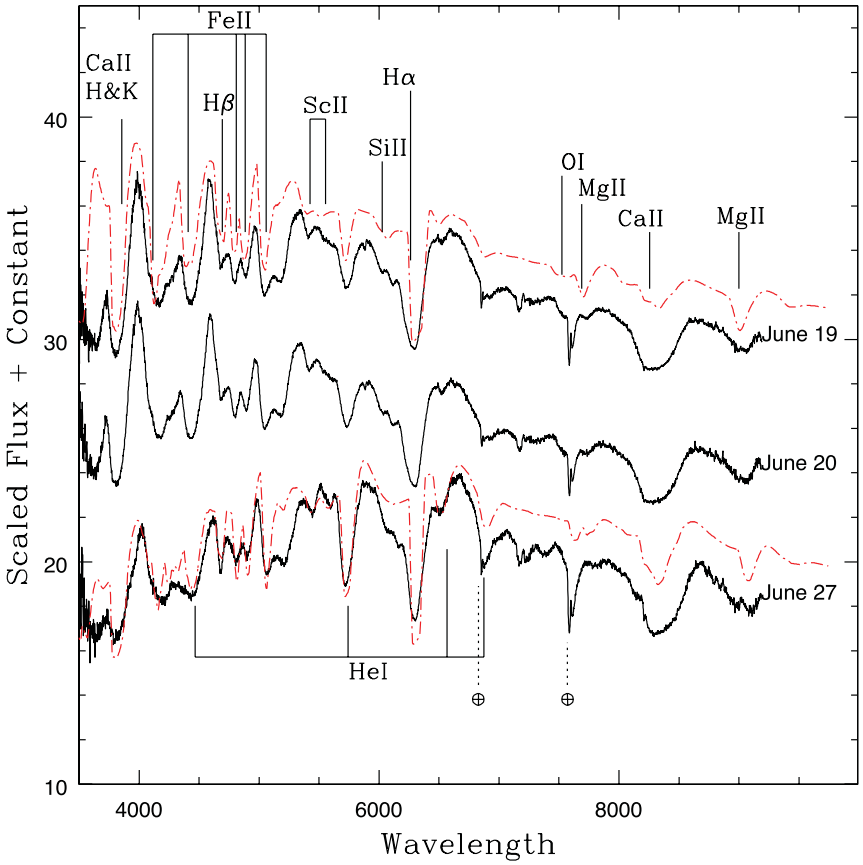

Figure 9. Spectral evolution of SN 2011dh during ∼20 to ∼27 d after explosion. The observed spectra (black) have been plotted with the synthetic spectra (red, dash–dotted) created using SYN++.

3.2.3 Transitional phase

The spectra of SN 2011dh during ∼41 to ∼99 d after explosion are shown in Fig. 11. A considerable evolution is seen in the spectrum during this period. The continuum becomes redder, the Balmer lines become sharper and have lower expansion velocities. The lines due to He I become stronger. The metamorphosis of SN 2011dh spectrum from Type II like to Type Ib like takes place during this period. The overall shape of the spectrum obtained on July 11 (day 41) is similar to the one obtained on June 27. The lines due to He I become stronger; P-Cygni features due to He I lines 4471, 5015, 5876, 6678, 7065 and 7281 Å are well developed. Hα line is weaker and narrower. The absorption components due to Ca II H&K and Ca II NIR triplet weaken, and the emission component of Ca II NIR becomes stronger. The [Ca II] 7291, 7324 Å feature starts appearing, blended with He I 7281 Å. The forbidden line [O I] at 5577 Å is also prominent.

The spectral evolution between July 11 and August 2 is very slow. The Hα absorption continues to weaken; the strength of the [Ca II] feature and Ca II NIR triplet increases. Except for the narrow Hα absorption, the spectrum of SN 2011dh displays all the features of Type Ib supernova. The emergence of forbidden lines due to calcium and oxygen shows that the spectrum is entering into nebular phase.

The spectrum of September 7 shows a complete transformation from type IIb to type Ib. The [O I] feature at 6300, 6363 is seen, while the Hα absorption has completely disappeared. The He I lines at 5876, 6678 and 7065 start weakening, the absorption component of Ca II NIR triplet becomes weaker, and the spectrum appears to be dominated by emission lines.

Synthetic spectra modelled with the SYN++ code is also plotted in Fig. 11, along with the observed spectra. There is not much evolution seen in the photospheric velocity and the photospheric temperature during this phase. The synthetic spectrum of July 11 has $T_{\rm bb} = 4300$ K and $v_{\rm phot} = 4500\,{\rm km\,s^{-1}}$. Hydrogen is still detached from the photosphere with $v_{\rm min} = 10\,500\,{\rm km\,s^{-1}}$, whereas helium is now undetached. The absorption bluewards of Hα can be fitted with Ba II 6142 and 6496 Å lines. The synthetic spectrum which fits the observed spectrum of September 7 has a very similar blackbody temperature and photospheric velocity as that of July 11, but no hydrogen.

The spectrum of SN 2011dh ∼60 d after explosion is compared with other Type IIb supernovae in Fig. 12. The overall appearance of the day 63 spectrum of SN 2011dh is very similar to the day 59 spectrum of SN 1993J. In the spectra of all the objects shown in the figure, the He I 5876 Å absorption is strong, but the absorption due to Hα has a varying strength. In SN 2011dh and SN 1993J the Hα absorption is narrow and sharp; SN 2003bg and SN 2001ig still show broad, strong absorption, and in SN 2008ax it is almost negligible. In SN 2009mg, Oates et al. (2012) have shown that the Hα absorption was considerably strong ∼60 d after explosion, and completely disappeared in ∼110 d spectrum. In SN 1996cb a narrow Hα absorption was seen till day 107, and nearly vanish by day 114 (Qui et al. 1999).

The transition from a hydrogen-dominated early phase spectra to He dominated late phase spectra is the characteristic feature of Type IIb supernovae. This can be interpreted as the presence of a thin envelope of hydrogen at the time of explosion of the progenitor star. However, it appears that the exact amount of hydrogen the

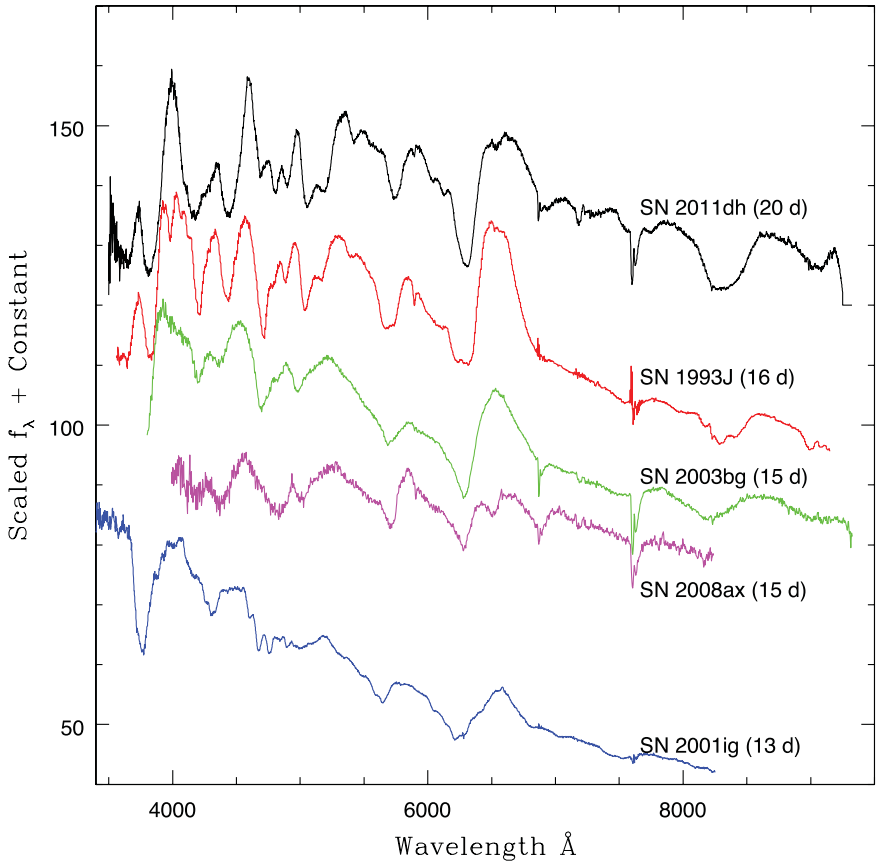

Figure 10. Comparison of spectra of SN 2011dh with those of SN 1993J, SN 2003bg, SN 2008ax and SN 2001ig during the early (close to maximum in *B* band) phase.

progenitors retain at the time of explosion differs significantly from object to object and mass of H envelope may play a key role in the photometric and spectroscopic evolution of these objects. The observed features of the light curve of SN 1993J are well reproduced by the explosion of a red supergiant whose H/He envelope mass has been decreased below $\sim$0.9 $M_\odot$ (Shigeyama et al. 1994). Woosley et al. (1994) arrived at the mass of hydrogen envelope as 0.2 $\pm$ 0.05 $M_\odot$. Using the late time spectra, Houck & Fransson (1996) estimated $\sim$0.3 $M_\odot$ as mass of hydrogen envelope in SN 1993J. Mazzali et al. (2009) have estimated mass of hydrogen layer as 0.05 $M_\odot$ for the broad-line Type IIb supernova SN 2003bg. In the case of SN 2008ax, Chornock et al. (2011) have estimated the mass of hydrogen envelope as $\sim$a few $\times$0.01 $M_\odot$. The overall similarity of the spectral evolution of SN 2011dh with SN 1993J indicates that the mass of the hydrogen envelope in SN 2011dh could be similar to that of SN 1993J. Indeed, Bersten et al. (2012) have shown that a progenitor star with He core of 3 to 4 $M_\odot$ with a thin hydrogen envelope of $\sim$0.1 $M_\odot$ can lead to a light curve similar to SN 2011dh.

3.2.4 Nebular phase

The next set of spectra were obtained when the supernova reappeared in the night sky, on 10 occasions, during 2011 November 20 to 2012 May 24. These spectra are shown in Fig. 13. The He I lines, which were prominent in the spectra obtained until 2011 September 7, are totally absent. Instead, the spectra are dominated by emission lines of Mg I] 4571 Å, [O I] 6300, 6363 Å, [Ca II] 7291, 7324 Å, O I 7774 Å, blend of [Fe II] lines at $\sim$5000 Å and the Ca II NIR triplet. The [O I] 5577 Å line had weakened, and almost disappeared in the spectrum of 2012 January 28. A bump, redwards of [O I] 6300, 6363 Å, is seen in all the late-phase spectra presented here.

In Fig. 14, the spectrum of SN 2011dh $\sim$6 months after explosion is compared with the spectra of SN 1993J, SN 2003bg and SN 1996cb at a similar epoch. Except for the difference in the strength of [Ca II] 7291, 7324 Å lines, all the spectra are similar. The flux ratio of the [Ca II] 7291+7324 and [O I] 6300+6363 lines is highest ($\sim$2) in SN 1996cb and the least ($\sim$0.2) in SN 1993J, while it is intermediate at a value of $\sim$0.8 and $\sim$0.5, respectively, in SN 2011dh and SN 2003bg. The bump redwards of [O I] 6300, 6363 Å line is seen in all the objects. During the early nebular phase, the observed bump may be the result of contribution from Fe II, [Fe II] and possibly [Co II] (Patat, Chugai & Mazzali 1995), and at least some part of the flux could arise from Hα scattering (Houck & Fransson 1996) also.

The spectrum of SN 2011dh obtained around $\sim$340 d after explosion is plotted along with the spectra of other well-studied Type IIb supernovae in Fig. 15. The common nebular features of all the supernovae are similar; however, there are some differences with respect to the relative strength of emission lines and their shapes. The Mg I]/[O I] line ratio at $\sim$280 d after explosion is $\sim$0.2 in SN 2011dh, $\sim$0.15 in SN 1993J and $\sim$0.36 in SN 2001ig, which is known to have the strongest Mg I] feature (Silverman et al. 2009). The strength of Hα (redwards of [O I] 6300, 6363 Å line) has increased, with the feature having a box-shaped profile, similar to that seen in SN 1993J, SN 2007Y and SN 2008ax.

The exact mechanism producing the late time Hα emission is not clearly known. However, the possible processes which can explain the late time Hα emission are: ionization of hydrogen by

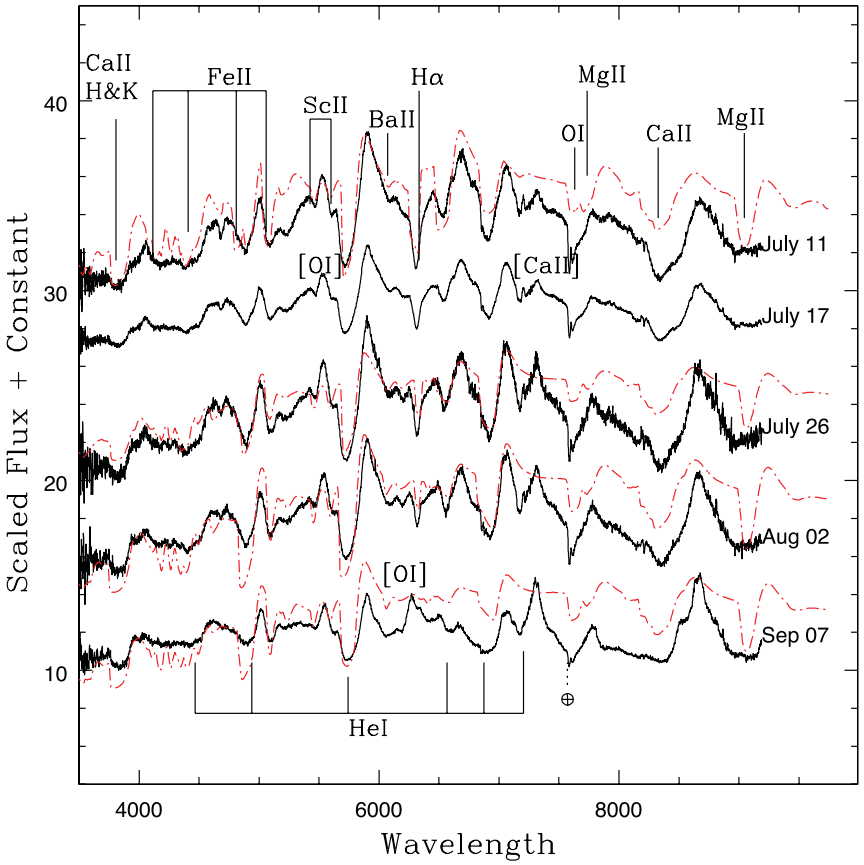

Figure 11. Spectral evolution of SN 2011dh during 41 to 99 d after explosion. The observed spectra (black) have been plotted with the synthetic spectra (red, dash–dotted) created using SYN++.

radioactivity and/or by the X-rays emitted due to the ejecta–wind interaction. For different objects, either of the two mechanisms may be operational. In SN 1993J, this feature was interpreted as due to Hα emission from a shell of hydrogen, possibly excited by interaction with a dense circumstellar medium (Patat et al. 1995; Houck & Fransson 1996). The observed late phase Hα emission in SN 2007Y was attributed to shock interaction by Stritzinger et al. (2009), but Chevalier & Soderberg (2010) proposed that the circumstellar density of SN 2007Y was too weak to produce the observed Hα luminosity through shock interaction, and hence radioactivity alone was the source for ionization of hydrogen. Taubenberger et al. (2011) have shown that the shock–wave interaction mechanism for late Hα emission from SN 2008ax faces serious problems in explaining the observed shape and velocity of the nebular Hα emission. An alternative mechanism, in which a right combination of mixing and clumping of hydrogen and helium is ionized by radioactive energy deposition has been shown to be able to reproduce the observed Hα emission in the late phase (Maurer et al. 2010).

Radio emission has been detected from SN 2011dh at a very early stage. It was detected at 86 GHz by the CARMA Radio Telescope $\sim$3 d after discovery (Horesh et al. 2011) and at 22 GHz $\sim$14 d after discovery (Marti-Vidal et al. 2011). This early phase radio emission is consistent with a non-thermal synchrotron self-absorbed spectrum of optical photons (Soderberg et al. 2012). SN 2011dh was monitored in the radio during late phases also with the VLBI. Based on these data a time-averaged expansion velocity of the forward shock was estimated as $21000 \pm 7000\,\mathrm{km\,s^{-1}}$ (Bietenholz et al. 2012). The observed X-ray emission from SN 2011dh gives a strong indication of the presence of circumstellar material, as the X-ray emission can be interpreted as due to the interaction of the blast wave with its surrounding circumstellar medium (Campana & Immler 2012). Based on the evidence for the presence of circumstellar material, and the high expansion velocity of forward shock, it appears that shock–wave interaction may be the most plausible mechanism for the late Hα emission in SN 2011dh. A detailed modelling is, however, required to ascertain this possibility.

The profile of the [O I] 6300, 6363 Å and [Ca II] 7291, 7324 Å lines during the nebular phase has been plotted in Fig. 16. The [Ca II] line has a single peak, whereas the [O I] line shows a double peak profile, with a $\sim$3000 km s^{-1} separation between the two peaks. Such a double peaked [O I] profile, with a separation of $\sim$3000 km s^{-1}, is seen in the late time spectra of many stripped-envelope CCSNe (Maeda et al. 2008; Taubenberger et al. 2009; Milisavljevic et al. 2010), and is interpreted as due to asphericity in the explosion with preferred viewing angle, as spherical explosion cannot produce the double peaked [O I] lines. However, Maurer et al. (2010) suggest that Hα absorption is probably responsible for the double peak profile of the [O I] doublet in several Type IIb supernovae. They have shown that Hα absorption causes a split of the [O I] doublet if it is located at around 12 000 km s^{-1}. The Hα line velocity evolution in SN 2011dh (Fig. 17) shows that it starts with $\sim$17500 km s^{-1} and flattens at $\sim$12 000 km s^{-1} after day 25, which looks consistent with the model suggested by Maurer et al. (2010). The spectra beyond day 173 show the emergence of Hα emission, which could be responsible for redwards asymmetry of [O I] profile (Figs 13–15). However, spectropolarimetric observation and detailed modelling are required to differentiate between

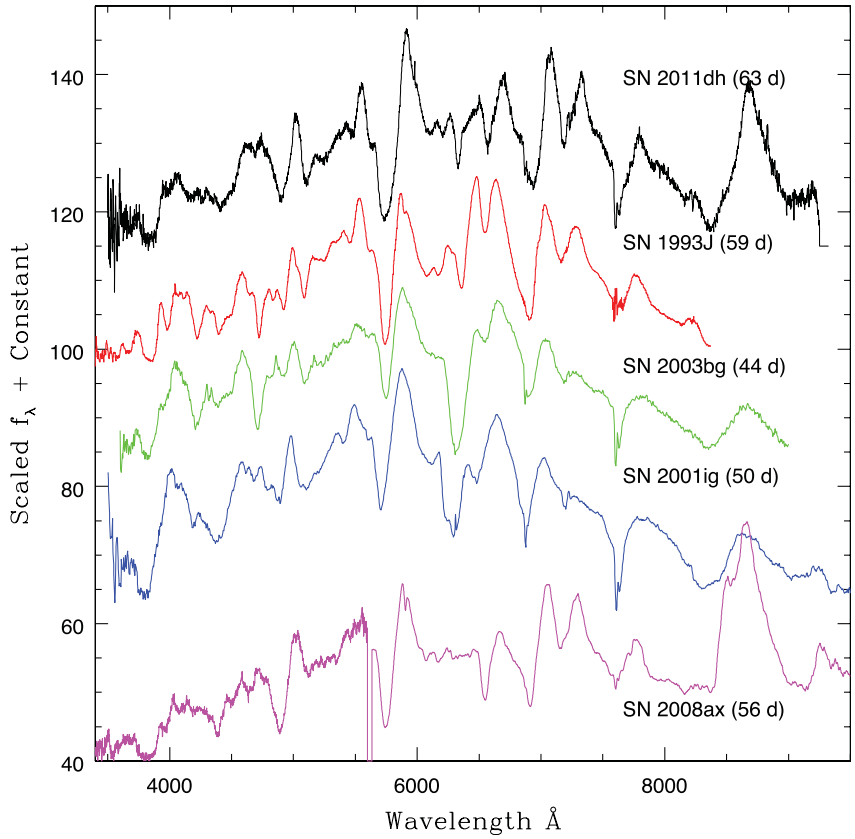

Figure 12. Comparison of the spectrum of SN 2011dh with those of SN 1993J, SN 2003bg, SN 2001ig and SN 2008ax at ∼2 months after explosion.

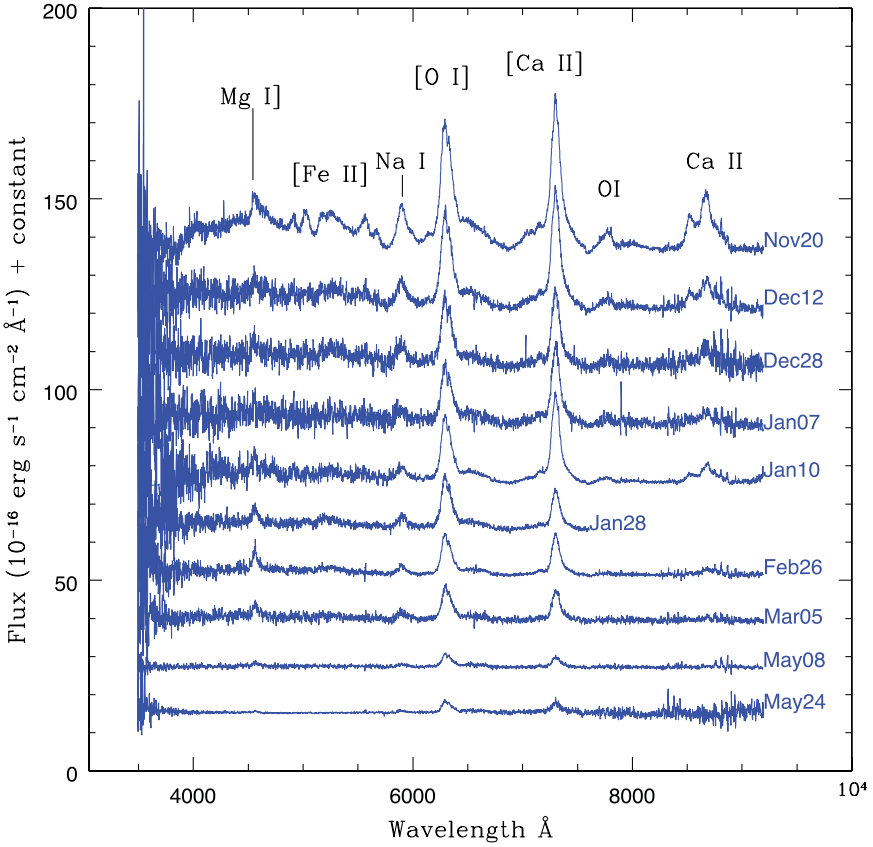

Figure 13. Spectral evolution of SN 2011dh during ∼173 to ∼360 d after explosion.

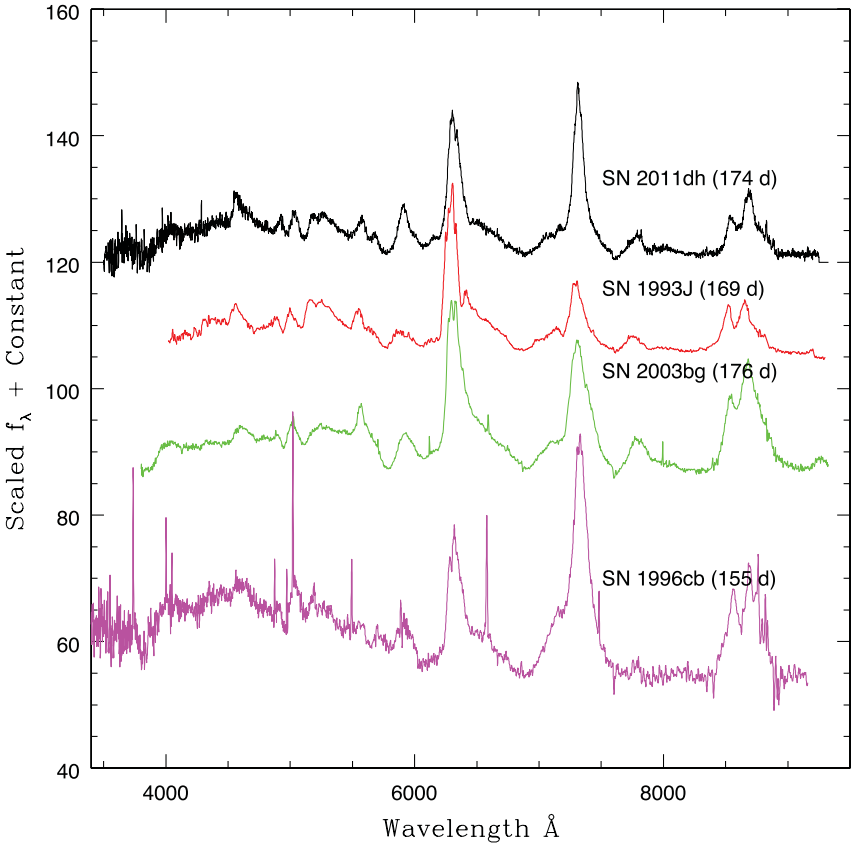

Figure 14. A comparison of the spectrum of SN 2011dh with those of SN 1993J, SN 2003bg and SN 1996cb at epoch ∼6 months after explosion.

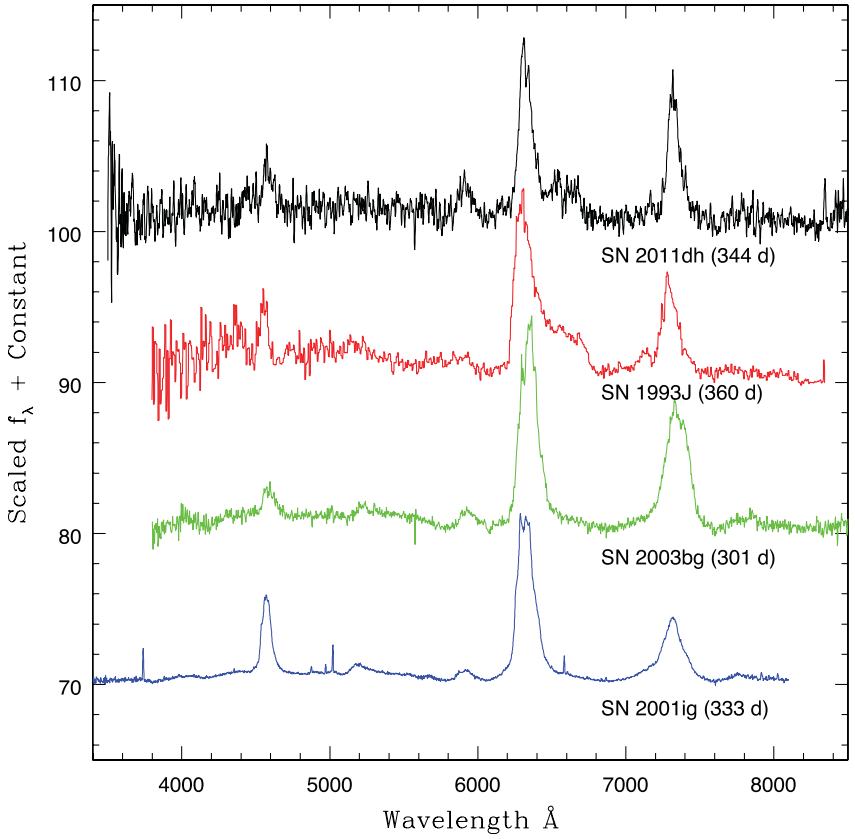

Figure 15. A comparison of the spectrum of SN 2011dh with those of SN 1993J, SN 2003bg and SN 2001ig at epoch ∼1 year after explosion.

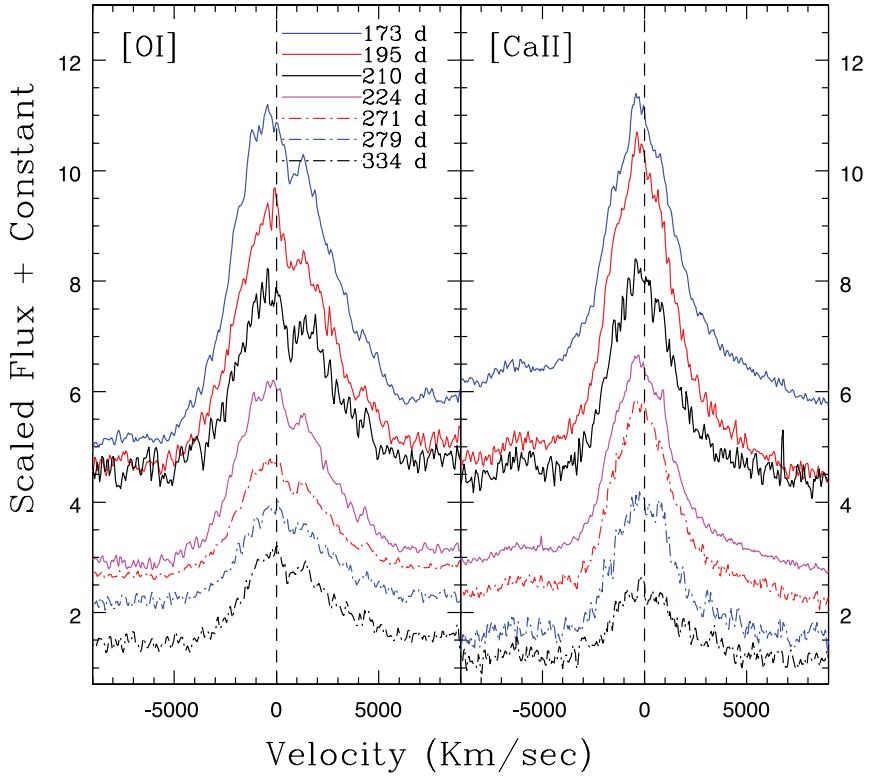

Figure 16. Line profile of [O I] λλ 6300, 6363 and [Ca II] λλ7291, 7324 lines during the nebular phase.

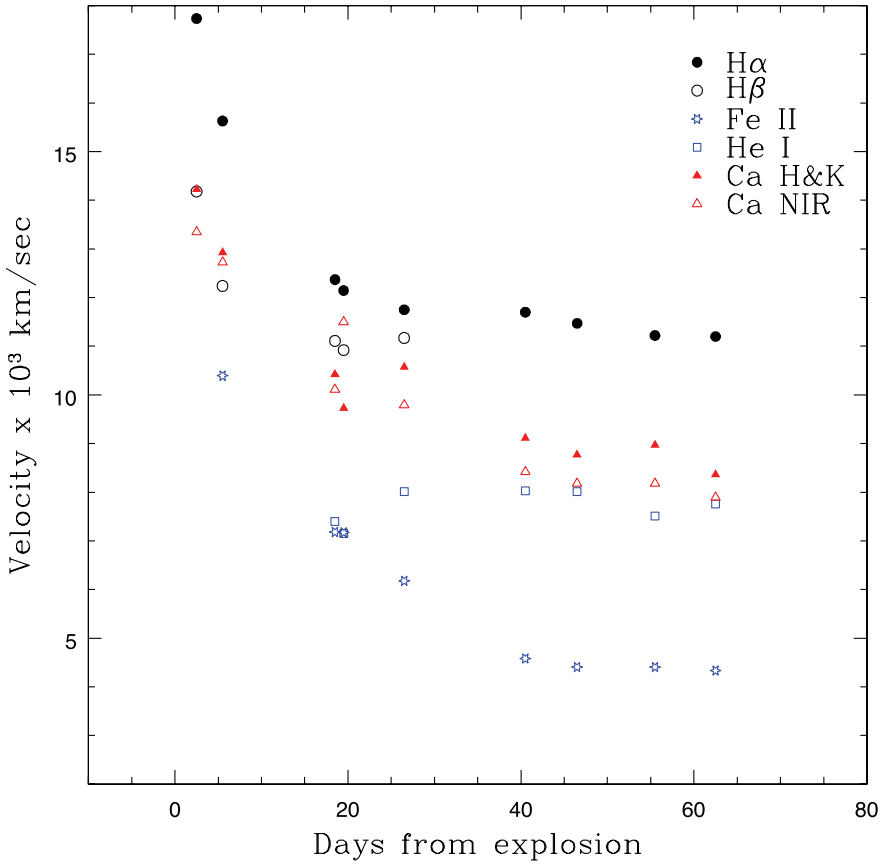

Figure 17. Evolution of the expansion velocity of supernova ejecta measured using different species.

asphericity and Hα as the cause of the double peak asymmetric profile.

3.2.5 Expansion velocity of the ejecta

Expansion velocity of the ejecta has been measured from the minima of P-Cygni profiles of relatively isolated lines, e.g. Hα, Hβ, He I 5876 Å and Fe II 5169 Å. For measuring the velocities, the absorption component of the P-Cygni profile was fitted with a Gaussian. The estimated line velocities are plotted in Fig. 17. The expansion velocity of Hα declines from $\sim$17500 km s^{-1} at $\sim$3 d after explosion to $\sim$12 000 km s^{-1} $\sim$19 d after explosion, and then remains almost constant. The Ca II H&K and Ca II NIR lines also show a similar trend; they decline from an initial velocity of $\sim$14 000 km s^{-1} to $\sim$10 000 km s^{-1}, $\sim$19 d after explosion, and remains almost constant thereafter. The expansion velocity of the ejecta measured using weak, unblended lines such as Fe II 5169 Å is often considered a good tracer of the photospheric velocity. The Fe II 5169 line velocity in SN 2011dh has an initial value of $\sim$10 000 km s^{-1} that declines until $\sim$40 d after explosion, and then flattens at $\sim$4500 km s^{-1}. We do not find much evolution in the velocity of the He I 5876 Å line, which shows a marginal increase from an initial value of $\sim$7000 km s^{-1} to $\sim$8000 km s^{-1} and remains almost constant at this value.

The measured expansion velocity $\sim$20 d after explosion shows three different representative velocities – the Hα line shows a higher velocity at $\sim$12 000 km s^{-1}, the Ca II H&K and Ca II NIR triplet lines are at $\sim$10 000 km s^{-1} and the Fe II line is at $\sim$7000 km s^{-1}. The velocity stratification becomes more prominent beyond day 40, with the Hα velocity being around 11 000 km s^{-1}, the He I 5876 Å and the Ca II H&K and Ca II NIR triplet at $\sim$8500 km s^{-1} and the Fe II 5169 Å line at a lower velocity of $\sim$4500 km s^{-1}. Assuming the supernova ejecta expands homologously, the three velocity groups indicate the ejecta to have three layers. The outermost layer is made of a thin hydrogen layer moving with high velocity, the intermediate, denser layer consists of Ca and probably He, and the innermost high-density core consisting of Fe and other heavy species is moving with lower velocity. A similar stratification of H and He layers is confirmed by spectral modelling of SN 2003bg (Mazzali et al. 2009), where the weaker Balmer lines level off at a velocity of $\sim$10 000 km s^{-1} and He I lines level off at a lower velocity $\sim$7000 km s^{-1}.

In Fig. 18 the measured line velocities of SN 2011dh are plotted with those of SN 1993J, SN 2003bg and SN 2008ax. The photospheric velocity as measured using the Fe II line and the helium layer velocity are very similar in all the supernovae. However, differences are seen in the Balmer line velocities. SN 2008ax and SN 2003bg have higher velocities, with the velocity at $\sim$40 d being $\sim$13 500 km s^{-1}, SN 2011dh at $\sim$12 000 km s^{-1} is intermediate, and SN 1993J has the lowest at $\sim$9500 km s^{-1}. A similar trend is seen in the evolution of the Hβ line velocity also. This may be related to the mass of the hydrogen envelope at the time of explosion, and the explosion energy. Iwamoto et al. (1997) have shown that for Type IIb supernovae, the minimum velocity of hydrogen depends mainly on the mass of the hydrogen envelope. This indicates that the mass of hydrogen envelope in SN 2011dh is between SN 1993J (0.2 to 0.9 M$_\odot$) and SN 2003bg (0.05 M$_\odot$). The estimate of hydrogen envelope mass of 0.1 M$_\odot$ in SN 2011dh by Bersten et al. (2012) agrees with this.

3.2.6 Oxygen mass and [Ca II]/[O I] ratio

The nebular spectra of stripped envelope CCSNe can be used to estimate mass of oxygen which is an indicator of the mass of the progenitor. Uomoto (1986) has shown that in the high-density limit ($N_e \geq 10^6$ cm^{-3}), the minimum mass of oxygen required to produce the observed [O I] emission can be estimated using the relation

$$M_O = 10^8 \times D^2 \times \mathrm{F([O\,I])} \times \exp^{(2.28/T_4)}, \quad (2)$$

where M_O is the mass of neutral oxygen in M$_\odot$, D is the distance in Mpc, F([O I]) is the flux of the [O I] 6300, 6364 Å line in erg s^{-1} and T_4 is the temperature of the oxygen emitting region in units of 10^4 K. Ideally, estimation of T_4 should be done using the flux ratio of [O I] 5577 Å to [O I] 6300−6364 Å lines. However, the presence of a weak [O I] 5577 Å line in the nebular spectra shows that the temperature in the oxygen emitting region is low and the limit of flux ratio [O I] 5577/6300−6364 can be assumed to be $\leq$0.1. In this limit, the emitting region will be either at high density ($N_e \geq 10^6$ cm^{-3}) and low temperature ($T_4 \leq 0.4$) or at low density ($N_e \leq 10^6$ cm^{-3}) and high temperature ($T_4 = 1.0$) (Maeda et al. 2007). For the few well-studied Type Ib supernovae, during the nebular phase, the oxygen emitting region is usually found to be of high density and low temperature (Schlegel & Kirshner 1989; Leibundgut et al. 1991; Elmhamdi et al. 2004). Using the observed flux of 1.03 × 10^{-13} erg s^{-1} cm^{-2} of [O I] 6300, 6364 Å line on 2012 February 26 and assuming that $T_4 = 0.4$ K holds good for SN 2011dh, the mass of oxygen is estimated as 0.22 M$_\odot$. There is a hint of the presence of [O I] 7774 Å line in the late phase spectra of SN 2011dh; this line arises mainly due to the recombination of ionized oxygen (Begelman & Sarazin 1986). Hence, it is appropriate to consider that some oxygen lies in an ionized form and the estimated mass of oxygen 0.22 M$_\odot$ is a lower limit of total mass of oxygen ejected during the explosion.

The estimate of mass of oxygen obtained, using a similar methodology, for some Type Ib/c supernovae indicates that it varies from $\sim$0.3 to 1.35 M$_\odot$ (Elmhamdi et al. 2004). For SN 2007Y, Stritzinger et al. (2009) have shown that in their model an oxygen mass of 0.2 M$_\odot$ reproduces the observed late time spectrum. Specifically, for type IIb events, Houck & Fransson (1996) arrived at an oxygen mass of $\sim$0.5 M$_\odot$ for SN 1993J by modelling the late time spectra, whereas modelling of early and late time spectra of SN 2003bg led Mazzali et al. (2009) to an oxygen mass estimate of 1.3 M$_\odot$. The mass of oxygen derived by modelling the late time spectra of SN 2001ig is $\sim$0.8 M$_\odot$ (Silverman et al. 2009). The oxygen mass estimated for SN 2011dh is smaller as compared to the well-studied type IIb events SN 1993J, SN 2003bg, and is similar to the mass ejected in the explosion of SN 2007Y.

Oxygen is ejected mostly from the oxygen layer formed during the hydrostatic burning phase, and so, the mass of oxygen ejected is very sensitive to the main-sequence mass of the progenitor. Thielemann, Nomoto & Hashimoto (1996) have made explosive nucleosynthesis calculation and predicted major nucleosynthesis yields for the progenitor mass of 13–25 M$_\odot$. They have shown that mass of ejected oxygen is 0.22, 0.43, 1.48 and 3.0 M$_\odot$ for progenitor mass of 13, 15, 20 and 25 M$_\odot$, respectively. Nomoto et al. (2006) have calculated nucleosynthesis yields of CCSNe and hypernovae models for 13–40 M$_\odot$ progenitor stars for various explosion energies and progenitor metallicity. For CCSNe of a progenitor mass 13 M$_\odot$, with the explosion energy of 1×10^{51} ergs and metallicity $Z = 0$, 0.001, 0.004 and 0.02, the mass of oxygen ejected in the explosion is 0.45, 0.50, 0.39 and 0.22 M$_\odot$, respectively. For similar explosion energy and metallicity range, the mass of oxygen for

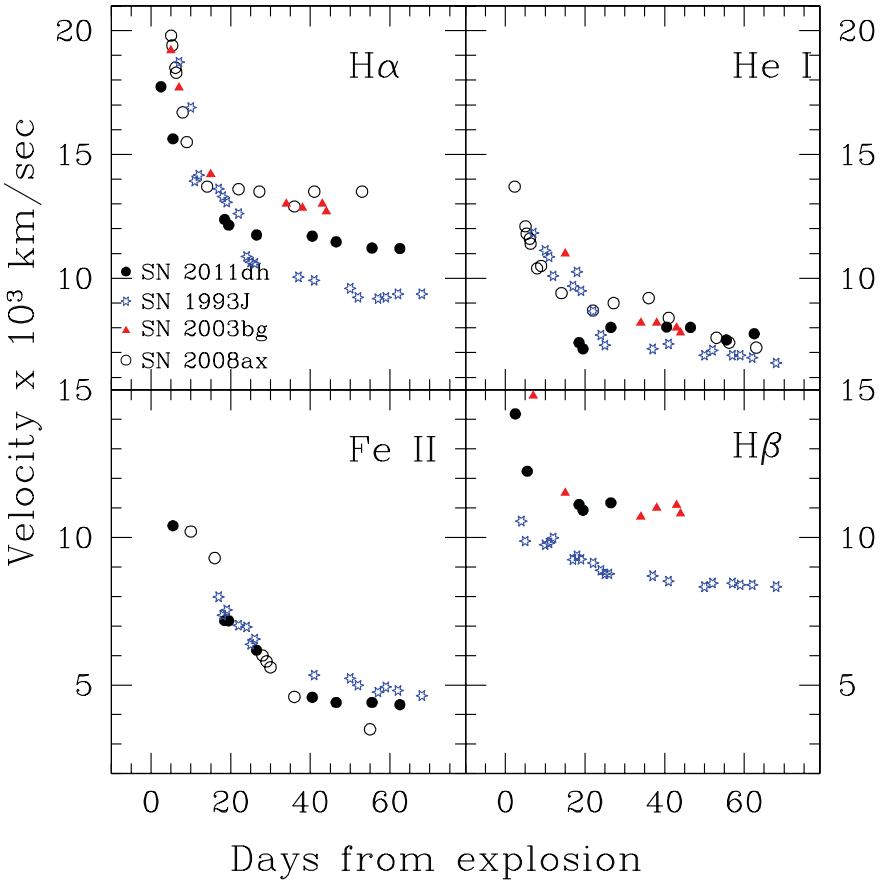

Figure 18. Comparison of the evolution of expansion velocity of SN 2011dh with those of SN 1993J, SN 2003bg and SN 2008ax.

a progenitor star of 15 $M_\odot$ is 0.77, 0.29, 0.29 and 0.16 $M_\odot$. The abundance analysis of H II regions in M51 by Bresolin, Garnett & Kennicutt (2004) has revealed that the O/H abundance is below the solar value for most of the H II regions studied. H II regions 53, 54 and 55 of Bresolin et al. (2004) are close to the location where SN 2011dh occurred. The measured 12 + log(O/H) values for these regions vary between 8.49 and 8.66 (considering the solar value as 8.69). It shows that the metallicity of the nearby H II regions is close to few tenths of that of solar. Assuming that the metallicity at the supernova location is similar to the nearby H II regions, the mass of the ejected oxygen estimated using the oxygen flux in the late time spectra indicates the progenitor of SN 2011dh to be a low-mass star of ∼13–15 $M_\odot$. The progenitor of a Type IIb supernova can be either a single massive star that had gone to Wolf–Rayet phase after losing most of its hydrogen-rich envelope before explosion, or it can be a less massive star in a binary system, being stripped off its hydrogen envelope during interaction with the binary component. The inferred lower mass of the progenitor suggests that the progenitor of SN 2011dh was likely a member of a binary system like the progenitor of SN 1993J (Podsiadlowski et al. 1993; Maund & Smartt 2009) and SN 2008ax (Roming et al. 2009; Taubenberger et al. 2011).

Fransson & Chevalier (1989) have theoretically calculated the ratio of flux of [Ca II] 7291–7324/[O I] 6300−6364 and shown that it weakly depends on the density and temperature of the emitting region, and is expected to remain relatively constant at late epoch. The flux ratio [Ca II] 7291–7324/[O I] 6300−6364 also serves as a good diagnostic of main-sequence mass of the progenitor star, as mass of oxygen ejected in the explosion depends on the progenitor mass and mass of Ca synthesized during the explosion is not sensitive to the main-sequence mass of the progenitor (Nomoto et al. 2006). Hence, a small value of the flux ratio is expected for massive progenitors. Elmhamdi et al. (2004) have investigated the evolution of observed [Ca II]7291–7324/[O I] 6300−6364 for some CCSNe during sufficiently late phases and shown that it remains fairly stable. The smaller value of [Ca II]/[O I] ratio for Type Ib/c supernova was explained as due to the absence of hydrogen-rich Ca II emitting region in them. For SN 2011dh, the [Ca II]7291–7324/[O I] 6300−6364 flux ratio at ∼340 and ∼360 d after explosion is found to ∼0.7, indicating that the progenitor star of SN 2011dh was a low-mass star. The flux ratio for SN 1993J, SN 2008ax and SN 2007Y at similar epochs is ∼0.5, 0.9 and 1.0, respectively.

Bersten et al. (2012) have computed hydrodynamical models based on evolutionary progenitors and shown that the early light curve of SN 2011dh can be reproduced with a large progenitor star with radius ∼200 $R_\odot$. In their modelling, based on the bolometric light curve and measured photospheric expansion velocity, mass of the ejecta, explosion energy and mass of ^{56}Ni was constrained to be ∼2 $M_\odot$, 6–10 × 10^{50} erg and 0.06 $M_\odot$, respectively. An explosion of a progenitor star with an He core of 3 to 4 $M_\odot$ and a thin hydrogen-rich envelope of ∼0.1 $M_\odot$ can lead to SN 2011dh like event. The progenitor star appears to be in a binary system with the main-sequence mass between 12 and 15 $M_\odot$. Benvenuto et al. (2013) have shown that evolution of a binary system with 16 $M_\odot$ + 10 $M_\odot$, and an initial period of 125 d, appears compatible with the pre-SN observations of SN 2011dh, and predicted that the yellow supergiant star detected in the pre-SN images could be the potential progenitor candidate. Our direct estimates of mass of ^{56}Ni using

the bolometric light curve, and property of the progenitor inferred using the mass of oxygen ejected in the explosion, the [Ca II]/[O I] ratio in the nebular phase and mass of hydrogen envelope are in very good agreement with the binary models.

4 CONCLUSIONS

In this paper, we present optical photometry in *UBVRI* bands and medium resolution spectroscopy of the Type IIb supernova SN 2011dh in nearby galaxy M51, during 3 d to one year after the explosion. SN 2011dh reached a peak absolute B magnitude of $M_B = -16.378 \pm 0.18$ with a rise time of 19.6 ± 0.5 d. With an absolute V peak magnitude of $M_V = -17.123 \pm 0.18$, SN 2011dh is ∼0.3 mag fainter than the mean absolute magnitude of a sample of Type IIb supernovae. The initial decline in magnitude within 15 d from the date of maximum (Δm_{15}) in the B and V bands is found to be similar to those of SN 1993J and SN 2008ax. In the late phase, between days 170 and 360, a steepening is seen in the B-band light curve, while the R and I bands show a flattening. This indicates the possibility of dust formation. The colour evolution shows that the $(B - V)$ and $(V - R)$ colours of SN 2011dh are always redder as compared to those of other stripped envelope CCSNe, which could be because of lower temperature of the supernova. Simple analytic fits to the bolometric light curve indicates that $\sim 0.09\,M_\odot$ of ^{56}Ni was synthesized in the explosion.

The early spectral evolution of SN 2011dh shows prominent P-Cygni absorption due to Balmer lines of hydrogen; the Hα absorption line is seen in the spectrum till ∼60 d after explosion. The He I lines start appearing in the spectrum much before the maximum in B band. Synthetic spectra have been computed using the SYN++ code and the main features in the spectra have been identified. The early photospheric temperature estimated at ∼7500 K is cooler than the estimates for other SNe IIb, indicating a more conducive condition for early dust formation. The emergence of forbidden lines due to [O I] 6300, 6363 Å and [Ca II] 7291, 7324 Å in the spectrum of ∼100 d after explosion indicates the onset of the nebular phase. The [O I] 6300−6364 line shows a double peaked profile. A box-shaped emission due to Hα is seen in the red wing of the [O I] line, which could possibly arise because of the shock–wave interaction of CSM. The ejected mass of oxygen ($\sim 0.22\,M_\odot$), estimated using the [O I] 6300, 6363 Å line flux, together with an intermediate value of the [Ca II] 7291–7324/[O I] 6300−6364 flux ratio suggests a less massive progenitor in a binary system.

ACKNOWLEDGEMENTS

We would like to thank the referee for a careful reading of the manuscript and constructive suggestions, which helped us in improving the manuscript. We thank all the observers of the 2-m HCT (operated by Indian Institute of Astrophysics), who kindly provided part of their observing time for observations of the supernova. We thank K. Nomoto and K. Maeda for useful discussion. This work has made use of the NASA/IPAC Astrophysics Data System and the NASA/IPAC Extragalactic Database (NED) which is operated by Jet Propulsion Laboratory, California Institute of Technology, under contract with the National Aeronautics and Space Administration.

REFERENCES

Arcavi I. et al., 2011a, Astron. Telegram, 3413, 1
Arcavi I. et al., 2011b, ApJ, 742, L18
Arnett W. D., 1982, ApJ, 253, 785
Barbon R., Benetti S., Cappellaro E. Patat F., Turatto M., Ijima T., 1995, A&AS, 110, 513
Begelman M. C., Sarazin C. L., 1986, ApJ, 302, L59
Benvenuto O. G., Bresten M. C., Nomoto K., 2013, ApJ, 762, 74
Bersten M. C. et al., 2012, ApJ, 757, 31
Bessell M. S., Castelli F., Plez B., 1998, A&A, 333, 231
Bietenholz M. F., Brunthaler A., Soderberg A. M., Krauss M., Zauderer B., Bartel N., Chomiuk L., Rupen M. P., 2012, ApJ, 751, 125
Branch D., Benetti S., Kasen D., Baron E., Jeffery D. J., Hatano K., 2002, ApJ, 566, 1005
Bresolin F., Garnett D. R., Kennicutt R. C., Jr, 2004, ApJ, 615, 228
Campana S., Immler S., 2012, MNRAS, 427, 70
Chevalier R. A., Soderberg A. M., 2010, ApJ, 711, L40
Chornock R. et al., 2011, ApJ, 739, 41
Crockett R. M. et al., 2008, MNRAS, 391, L5
Elmhamdi A., Danziger I. J., Cappellaro E., Della Valle M., Gouiffes C., Phillips M. M., Turatto M., 2004, A&A, 426, 963
Elmhamdi A., Danziger I. J., Branch D., Leibundgut B., Baron E., Kirshner R. P., 2006, A&A, 450, 305
Filippenko A. V., 1988, AJ, 96, 1941
Filippenko A. V., 1997, ARA&A, 35, 309
Filippenko A. V., Matheson T., Ho L. C., 1993, ApJ, 415, L103
Fisher A., 2000, PhD thesis, Univ. of Oklahoma
Fransson C., Chevalier R. A., 1989, ApJ, 343, 323
Gal-Yam A. et al., 2007, ApJ, 656, 372
Griga T. et al., 2011, Central Bureau Electron. Telegrams, 2736, 1
Hamuy M., 2003, ApJ, 582, 905
Hamuy M. et al., 2009, ApJ, 703, 1612
Heger A., Fryer C. L., Woosley S. E., Langer N., Hartmann D. H., 2003, ApJ, 591, 288
Horesh A. et al., 2011, Astron. Telegram, 3411
Horne K., 1986, PASP, 98, 609
Houck J. C., Fransson C., 1996, ApJ, 456, 811
Iwamoto K., Young T. R., Nakasato N., Shigeyama T., Nomoto K., Hachisu I., Hideyuki S., 1997, ApJ, 477, 865
Jeffery D. J., Branch D., 1990, in Wheeler J. C., Piran T., Weinberg S., eds, Supernovae, Supernovae, Jerusalem Winter School for Theoretical Physics, Vol. 6, World Scientific, Singapore, p. 149
Krauss M. I. et al., 2012, ApJ, 750, L40
Kumar B. et al., 2013, MNRAS, 431, 308
Landolt A. U., 1992, AJ, 104, 340
Leibundgut B., Kirshner R. P., Pinto P. A., Rupen M. P., Smith R. C., Gunn J. E., Schneider D. P., 1991, ApJ, 372, 531
Lewis J. R. et al., 1994, MNRAS, 266, 27
Li W. et al., 2008, Central Bureau Electron. Telegrams, 1290, 1
Maeda K. et al., 2007, ApJ, 666, 1069
Maeda K. et al., 2008, Sci, 319, 1220
Marion G. H. et al., 2011, Astron. Telegram, 3435
Marion G. H. et al., 2013, preprint (arXiv:1303.5482)
Marti-Vidal I. et al., 2011, A&A, 535, L10
Maund J. R., Smartt S. J., 2009, Sci, 324, 486
Maund J., Smartt S., Kudritzki R., Podsiadlowski P., Gilmore G., 2004, Nat., 427, 129
Maund J. R. et al., 2011, ApJ, 739, L37
Maurer I., Mazzali P. A., Taubenberger S., Hachinger S., 2010, MNRAS, 409, 1441
Mazzali P. A., Deng J., Hamuy M., Nomoto K., 2009, ApJ, 703, 1624
Milisavljevic D., Fesen R. A., Gerardy C. L., Kirshner R. P., Challis P., 2010, 709, 1343
Milisavljevic D. et al., 2013, ApJ, 767, 71
Murphy J. W., Jennings Z. G., Williams B., Dalcanton J. J., Dolphin A. E., 2011, ApJ, 742, L4
Nadyozhin D. K., 1994, ApJS, 92, 527
Nomoto K., Tominaga N., Umeda H., Kobayashi C., Maeda K., 2006, Nucl. Phys. A, 777, 424
Nugent P., Branch D., Baron E., Fisher A., Vaughan T., Hauschildt P. H., 1995, Phys. Rev. Lett., 75, 394
Oates S. R. et al., 2012, MNRAS, 424, 1279

Pastorello A. et al., 2008, MNRAS, 389, 955
Pastorello A. et al., 2009, MNRAS, 394, 2266
Patat F., Chugai N., Mazzali P. A., 1995, A&A, 299, 715
Podsiadlowski Ph., Hsu J. J. L., Joss P. C., Ross R. R., 1993, Nat, 364, 509
Prabhu T. P. et al., 1995, A&A, 295, 403
Qiu Y., Li W., Qiao Q., Hu J., 1999, AJ, 117, 736
Richardson D., Branch D., Baron E., 2006, AJ, 131, 2233
Richmond M. W., Treffers R. R., Filippenko A. V., Paik Y., Leibundgut B., Schulman E. Cox C. V., 1994, AJ, 107, 1022
Ritchey A. M., Wallerstein G., 2012, ApJ, 48, L11
Roming P. W. A. et al., 2009, ApJ, 704, L118
Ryder S. D., Murrowood C. E., Stathakis R. A., 2006, MNRAS, 369, L32
Schlegel E. M., Kirshner R. P., 1989, AJ, 98, 577
Schlegel D. J., Finkbeiner D. P., Davis M., 1998, ApJ, 500, 525
Shigeyama T., Suzuki T., Kumagai S., Nomoto K., Saio H., Yamaoka H., 1994, ApJ, 420, 341
Silverman J. M., Mazzali P. A., Chornock R., Filippenko A. V., Clocchiatti A., Phillips M. M., Ganeshalingam M., Foley R. J., 2009, PASP, 121, 689
Silverman J. M., Filippenko A. V., Cenko S. B., 2011, Astron. Telegram, 3398, 1
Smartt S. J., 2009, ARA&A, 47, 63
Sobolev V. V., 1957, SvA, 1, 678
Soderberg A. M. et al., 2012, ApJ, 752, 78
Stalin C. S., Hegde M., Sahu D. K., Parihar P. S., Anupama G. C., Bhatt B. C., Prabhu T. P., 2008, Bull. Astron. Soc. India, 36, 111
Stritzinger M. et al., 2002, AJ, 124, 2100
Stritzinger M. et al., 2009, ApJ, 696, 713
Taubenberger S. et al., 2009, MNRAS, 397, 677
Taubenberger S. et al., 2011, MNRAS, 413, 2140
Thielemann F. K., Nomoto K., Hashimoto M. A., 1996, ApJ, 460, 408
Thomas R. C., Nugent P. E., Meza J. C., 2011, PASP, 123, 237
Tsvetkov D. Yu., Volkov I. M., Sorokina E. I., Blinnikov S. I., Pavlyuk N. N., Borisov G. V., 2012, Perem. Zvezdy, 32, 6
Uomoto A., 1986, ApJ, 310, L35
Van Dyk S. D. et al., 2011, ApJ, 741, L28
Vinko J. et al., 2004, A&A, 427, 453
Vinko J. et al., 2012, A&A, 540, 93
Wada T., Uneo M., 1997, AJ, 113, 231
Woosley S. E., Pinto P. A., Martin P. G., Weaver T. A., 1987, ApJ, 318, 664
Woosley S. E., Eastman R. G., Weaver T. A., Pinto P. A., 1994, ApJ, 429, 300
Yamanaka M., Itoh R. Ui T., Arai A., Nagashima M., Kajiawa K., 2011, Central Bureau Electron. Telegrams, 2736, 6

This paper has been typeset from a TEX/LATEX file prepared by the author.